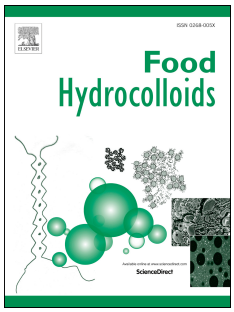

Experimental and modeling approaches applied to the whey proteins and vitamin B9 complexes study

Rocío Corfield, Gabriel Lalou, Santiago Di Lella, Karina D. Martínez, Carolina Schebor, Mariana C. Allievi, Oscar E. Pérez

PII: S0268-005X(23)00380-6

DOI: https://doi.org/10.1016/j.foodhyd.2023.108834

Reference: FOOHYD 108834

To appear in: *Food Hydrocolloids*

Received Date: 27 December 2022

Revised Date: 19 April 2023

Accepted Date: 26 April 2023

Please cite this article as: Corfield, Rocí., Lalou, G., Di Lella, S., Martínez, K.D., Schebor, C., Allievi, M.C., Pérez, O.E., Experimental and modeling approaches applied to the whey proteins and vitamin B9 complexes study, *Food Hydrocolloids* (2023), doi: https://doi.org/10.1016/j.foodhyd.2023.108834.

CrediT author statement

Rocío Corfield: Investigation, Validation, Formal analysis, Writing- Original draft, Visualization. **Gabriel Lalou*:*** Investigation, Software, Formal analysis, Writing- Original draft **Santiago Di Lella:** Investigation, Formal analysis, Writing- Original draft. **Karina Martínez:** Investigation, Formal analysis. **Carolina Schebor:** Investigation, Formal analysis, Supervision, Resources, Writing- Reviewing and Editing. **Mariana Allievi:** Investigation, Formal analysis, Methodology, Resources, Supervision, Writing- Reviewing and Editing. **Oscar E. Pérez**: Conceptualization, Methodology, Resources, Funding acquisition, Supervision, Writing- Reviewing and Editing**.**

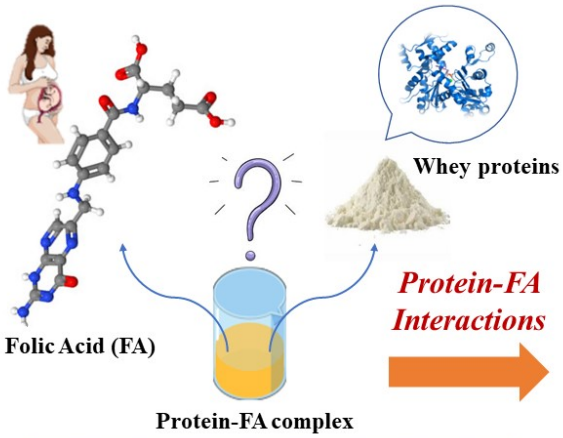

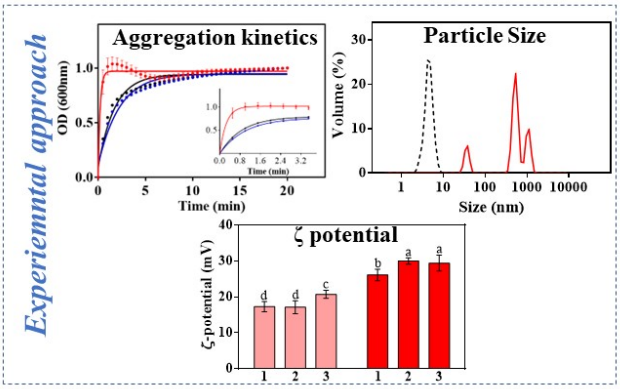

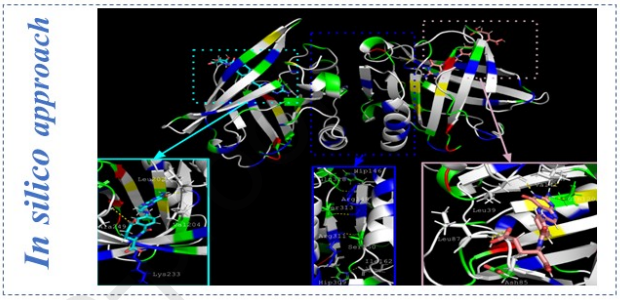

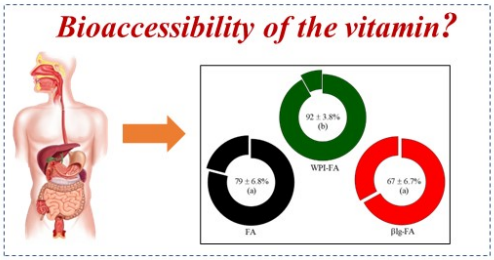

Experimental and modeling approaches applied to the whey proteins and vitamin B9 complexes study

Rocío Corfield[a,1], Gabriel Lalou[b,c,1], Santiago Di Lella[b,e], Karina D. Martínez[d,e], Carolina Schebor[a,e], Mariana C. Allievi[b,e*], Oscar E. Pérez[b,e*]

[a]*Consejo Nacional de Investigación Científica y Técnicas de la República Argentina, ITAPROQ-CONICET. Universidad de Buenos Aires. Departamento de Industrias, Facultad de Ciencias Exactas y Naturales. Intendente Güiraldes, s/n, Ciudad Universitaria. Buenos Aires, Argentina. CP 1428.*

[b]*Consejo Nacional de Investigación Científica y Técnicas de la República Argentina, IQUIBICEN-CONICET. Universidad de Buenos Aires, Departamento de Química Biológica, Facultad de Ciencias Exactas y Naturales. Intendente Güiraldes, s/n, Ciudad Universitaria. Buenos Aires, Argentina. CP 1428.*

[c]*Ecole Normale Supérieure Ulm, Paris Sciences et Lettres, Département de Chimie, 45 rue d'Ulm, F-75230 Paris cedex 05.*

[d]*Consejo Nacional de Investigación Científica y Técnicas de la República Argentina, ITPN-CONICET. Universidad de Buenos Aires. Facultad de Ingeniería. Las Heras 2214, Buenos Aires, Argentina. CP 1127.*

[e]*Members of CONICET, Argentina.*

[1]Both author contributed equally to this work

*To whom correspondence should be addressed

E-mail address: oscarperez@qb.fcen.uba.ar mallievi@qb.fcen.uba.ar

ABSTRACT

In this work, complexes of β-lactoglobulin (βlg) or whey protein isolate (WPI) with folic acid (FA) were developed as potential food ingredients. A dilute concentrations regime was employed to elucidate possible binding sites of the vitamin on the protein. The ζ potential, the aggregation kinetics and the particle size distributions were studied. On the other hand, *in silico* studies were carried. Additionally, the ability of the mixed systems to preserve the vitamin bioaccessibility was assessed by exposing the protein-FA systems to *in vitro* digestion. The ζ potential study showed similar values for the pure proteins and the mixed systems, obtaining for the highest concentrations studied (0.01825% W/W) values of: 21 ± 1 and 29 ± 2 mV for βlg and βlg-FA, and 22 ± 1 and 23 ± 2 mV for WPI and WPI-FA. These results suggest that the interactions between FA and proteins are of the hydrophobic type. The aggregation kinetics showed that the process of formation of protein-FA was slower than the formation of pure FA crystals. The particle size distributions showed different sizes between the pure proteins and those of the mixed systems. Regarding *in silico* studies, it was found that βlg presents regions where hydrogen bonding interactions between FA and certain amino acids of the protein prevail. Finally, regarding the bioaccessibility of the vitamin, WPI-FA was the system that obtained the highest value (92%). These complexes could be used as ingredients to be incorporated into foods consumed by people with special diets such as pregnant women.

Keywords: Folic acid, β-lactoglobulin, whey protein isolate, complexation, dimer equilibrium, bioaccessibility.

1. Introduction

Proteins are interesting chemical building blocks for encapsulation methodologies of high efficacy due to their ability to form protein-ligand complexes, protecting the bound active substances against oxidation and degradation, and providing means of controlled release (De Wolf & Brett, 2000; Zhang, Subirade, Zhou, & Liang, 2014; Li, Wang, Hu, Wu & Van der Meeren, 2022a). In this context, β-lactoglobulin (βlg) is a globular protein with a molecular weight of 18.4 kDa which contains several binding sites, allowing the interaction with various ligands of different types (Paul, Ghosh & Mukherjee, 2014; Zhang et al., 2022). βlg monomer consists of 162 amino acids, including a free cysteine and two disulfide bridges (Cys106-Cys119 and Cys66-Cys160) (Sengupta, Das & Sen, 2018; Farooq et al., 2019;). This protein has shown a great ability to protect different compounds of high biological value against heat, oxidation, and irradiation (Makori, Mu & Sun, 2021; Qie et al., 2021; Zhang et al., 2022; Zhang, Lu, Zhao, Wang, Wang & Zhang, 2022). On the other hand, milk whey is widely used as a food ingredient, containing 20% of the total proteins of milk (Al-Jasaar, Mikajiri & Roos, 2020), being β-lactoglobulin, α-lactalbumin, and BSA, the 80% of whey protein content (Carter & Drake, 2018; Halabi et al., 2020). In this context, whey protein isolates (WPI) and whey protein concentrates (WPC), are currently of great interest due to their versatility to transport molecules of biological interest (Tang, 2021).

Vitamin B9 (Vit B9) is very important in nutrition and health since its deficiency has a direct impact on different metabolic pathways, being the most problematic issue the one related to nucleotides synthesis. Accordingly, its deficiency has been related to various health complications such as cardiovascular diseases, colon cancer, neurocognitive impairment, and neural tube defects during embryos development (Scholl & Johnson, 2000; Assanelli et al., 2004; Pérez, David-Birman, Kesselman, Levi-Tal, Lesmes, 2014; Ruiz-Rico et al., 2017, Mohammed, Dyab, Taha & Abd-El-Mageed, 2021). In this sense, FAO & WHO (2004) recommend a daily consumption of 400 μg of Vit B9 for people in good health and for the case of people undergoing treatment against macrocytic nutritional anemia, or to prevent neural tube defects in pregnant women, the recommended daily dose is 5 to 10 mg. In consequence, to ensure the consumption of this vitamin, a synthetic folate, i.e. folic acid (FA), is used to fortify foods. FA is more stable compared to natural folates. However, significant FA losses have been reported during food processing and storage (Gazzali et al 2016). Neves et al. (2019) studied the stability of FA in a fortified French bread and found losses of 39% after baking. Frommherz et al. (2014) studied the storage of FA-fortified orange juices for 12 months and reported that

after one-month occurred the highest rate of degradation due to oxygen remaining in the container headspace.

Recently our research group established a simple methodology to develop a food ingredient composed of milk whey proteins and FA, more specifically: βlg and WPI. The use of WPI allowed the generation of a low-cost protein based FA ingredient, having similar characteristics to the complexes prepared with pure βlg (Corfield et al., 2020). The methodology proposed to generate whey protein-FA complexes would be a solution to ensure the stability of this vitamin. Our previous study was focused on the aggregation phenomena occurring at low pH when mixing concentrated protein-FA solutions, i.e. concentrated regime. In this opportunity, our objective was to deepen the knowledge about the interactions occurring between the proteins (βlg and WPI) and FA. With this aim, a diluted regimen was employed, and the focus was put on elucidating possible binding sites of the vitamin on the protein molecule and find the prevailing complex structures in the protein-FA mixed systems. Another purpose of this research was to evaluate if the FA present in the mixed systems preserved its bioaccessibility after applying an *in vitro* human gastrointestinal digestion model. These objectives were faced through experimental and modeling approaches. The obtained information may help to design new ingredients/carriers for FA.

2. Materials and Methods

2.1. Materials

FA, 99.0 % purity, was kindly given by Laboratorios Bagó (La Plata, Argentina); β-lactoglobulin (β-lg) >97.0 % was supplied by Davisco Foods International, Inc. (Le Sueur, Minnesota); whey protein isolate (WPI) >90% protein was provided by Arla Foods Ingredients S.A. (Buenos Aires, Argentina); MRS medium of Biokar, (Beauvais, France), Folic Acid Casei Medium (FACM) of Difco (Argentina). All reagents were of analytical grade.

2.2. Protein-FA mixed systems

The protein-FA mixed solutions were prepared following the methodology previously used Corfield et al. (2020) with some modifications. Briefly, βlg or WPI stock solutions were prepared in concentrations of 0.0125%; 0.0250% and 0.0365% (g of dissolved powder/100 g of solution) which were allowed to hydrate for 24 h at 4 °C. On the other hand, FA stock solutions were prepared at 0.0125, 0,0250 and 0,0365% (g of dissolved powder/100 g of solution). Finally, protein stock solutions at pH 7.0 (βlg or WPI) and FA stock solutions at pH

7.0, were mixed in equal weight obtaining the final mixtures of protein-FA with concentrations of 0.00625; 0.0125 and 0.01825 g for each dissolved species/100 g of solution. The resulting mixed solutions were adjusted to pH 3.0 using citric acid according to Corfield et al. (2020). Following the same procedure, the pertinent controls of pure protein and pure FA were prepared.

2.3. Physicochemical characterization

2.3.1. ζ – potential

ζ-potential was registered following the methodology of Martínez et al. (2019). The process consisted in 12 sequential readings at 25 °C, placing the samples in disposable capillary cells (DTS1060, Malvern Instruments, Worcestershire, United Kingdom), using a Zetasizer Nano-Zs analyzer, from Malvern Instruments (Worcestershire, United Kingdom). Results were expressed as the mean of three replicates ± the standard deviation.

2.3.2. Surface hydrophobicity

The surface hydrophobicity (S_0) of the βlg and WPI and βlg-FA and WPI-FA complexes were analyzed using 1-anilino-8-naphathalene-sulfonate (ANS, Sigma-Aldrich Inc., St Louis, MO, USA) according to the method of Pérez et al. (2014) with some modifications. Briefly, as indicated in **item 2.2**, serial solutions of the protein control solutions (βlg or WPI) and βlg -FA or WPI-FA complexes solutions were prepared in a concentration range of 0.00228-0.0365%. Subsequently, 3 ml of each solution was mixed with 15 µl of ANS (8.0 mM phosphate buffer 0.01 M, pH 7.0). The fluorescence intensity (FI) of the ANS was determined at a wavelength of 480 nm with excitation at 380 nm using a Cary Eclipse fluorescence spectrophotometer (Agilent Technologies, USA). Finally, S_0 for each system was calculated as the slope of the plot of the FI vs. protein concentration.

2.3.3. Particle size distribution

The analysis of particle size distribution was carried out by dynamic light scattering (DLS) following the procedure described by Carpineti, Martínez, Pilosof & Pérez (2014), using the same device described in 2.3.1. Measurements were made at 25 °C and at a fixed angle of 173°, within a range of 0.6 nm to 6 µm, according to the equipment specifications. Ten readings were taken from each sample (n= 3), contained in a disposable polystyrene cuvette. The intensity distribution was determined using a multiple exponential function (CONTIN), which was used to analyze the percent distribution data of particle/aggregate sizes (Štěpánek, 1993). The global

particle size distribution was evaluated, and the main peaks and the polydispersity index (PId) were analyzed according to Ochnio et al. (2018).

2.3.4. Aggregation kinetics

The kinetics of aggregation was analyzed according to Prudkin-Silva et al. (2018) with some modifications. The association of proteins with FA was analyzed by following the increase in absorbance over time at 600 nm at 25°C for 20 min, using a JASCO V 630 UV-Visible spectrophotometer (Tokyo, Japan). The samples were prepared directly into the quartz cuvette by mixing the required solutions volume to generate de systems detailed in 2.2. The curves obtained were normalized and fitted according to Stirpe et al. (2011) with minimal modifications, using an exponential function:

$$OD(t) = OD_{\infty} - \Delta OD \ exp(-Kt) \qquad \textbf{(Eq. 1)}$$

Where OD is the optical density value at time t; OD∞ is the final optical density value, ΔOD is the optical density amplitude, and K is the rate of aggregate formation.

2.4. *Flexible Docking and Molecular Dynamics Simulation (MDS)*

2.4.1. System preparation for MD simulations

Coordinates for the βlg were retrieved from the Protein Data Bank (PDBid= 1BSY.pdb). Protein systems were built for two pH values, 3.0 and 7.0. The difference between the systems at both pHs was reflected by the protonation state of the ionizable residues. The PROPKA algorithm (Li, Robertson & Jensen, 2005) was used and final coordinates for the protein atoms were obtained with the H++ version 4.0 (Bashford & Karplus, 1990) server, estimating the protonation states at two pHs, 3.0 and 7.0. Differences between the systems in both states were found for Asp33, 53, 64, 85, 129, 137 and Glu44, 45, 51, 55, 62, 65, 74, 89, 112, 114, 127, 131, 134, 158. All the histidine residues were found to be fully protonated (positively charged) for both pHs. Both systems were modeled with the Amber ff14SB force field (Maier et al., 2015). The systems were solvated with the TIP3P water model (Jorgensen, Chandrasekhar, Madura, Impey & Klein, 1983) using the tLeAP module of the Amber 20 simulation suite (Case et al., 2020), in octahedral boxes using a distance of 10 Å from the protein surface, resulting in the addition of approximately 6,000 TIP3P residues for the systems, respectively. A physiological salt concentration of 0.15 M was achieved through the addition of Na^+ and Cl^- ions, after

neutralizing the system charge in each case (protein pH 7.0: –7e; protein pH 3.0: +16e). Hydrogens and other atoms not resolved in the cryo EM structures as well as the disulfide bonds were added using the tLeAP module of the Amber 20 simulation suite (Case et al., 2020).

2.4.2. MD simulations and checking protocols

To predict the βlg-FA complex/dimer structure, the first step of our study was to perform all-atom MDS of the protein alone at pH 7.0 and pH 3.0, as followed by the protonation state of the residues mentioned above. Each system was subjected to 5000 steps of steepest descent minimization followed by 5000 steps of a conjugated gradient, further heating from 0 to 100 K over 45 ps with a 0.5 fs time step with restrains (10 $kcal.mol^{-1}.Å^{-2}$) applied to all protein atoms, and then heating from 100 to 300 K over 45 ps with a 1 fs time step with the same restraints on the protein. The system was then equilibrated for additional 200 ps at constant temperature and volume with all atoms restraints (10 $kcal.mol^{-1}.Å^{-2}$), followed with a 200 ps lower restraints (5 $kcal.mol^{-1}.Å^{-2}$) equilibration with the same parameters. After another 200 ps equilibration at constant temperature and pressure with backbone lower restraints (5 $kcal.mol^{-1}.Å^{-2}$), the system was finally equilibrated for 200 ps without restraints. For constant pressure simulations, isotropic position scaling was performed with the Berendsen barostat and a pressure relaxation time of 2.0 ps. The Langevin thermostat was used with a collision frequency of 5.0 ps^{-1} (Uberuaga, 2004; Sindhikara, Kim, Voter & Roitberg, 2009). The SHAKE algorithm was used to constrain bonds to nonpolar hydrogens (Ryckaert, Ciccoti & Berendsen, 1977). A 10.0 Å cutoff was used for nonbonded interactions.

Three replicas of a 300 ns production were conducted with different initial sets of velocities, under the same NVT conditions described above but with collision frequency of 5.0 ps^{-1} a 2.0 fs timestep, using the PMEMD cuda module of the Amber 20 simulation suite (Case et al., 2020). Coordinates were saved on disk every 40ps for subsequent analysis. Trajectory analysis was performed using the CPPTRAJ module of the Ambertools 20 package of programs. Temperature and energy profiles were checked for every MD simulation. In order to check the convergence of the trajectory, Root Mean Square Deviation (RMSD) and Root Mean Square Fluctuations (RMSF) were computed after identifying the lowest potential energy structure (**Figure 1-SM**). Clusterization was conducted with the k-means algorithm (Shao, Tanner, Thompson & Cheatham, 2007). Interaction analysis focused on the most populated clusters after the production. The time evolution of cluster population for each structure is given in **Figure 2-SM**.

2.4.3. Docking and MDS on complex/dimer structures

The structures obtained after clustering were then used in a docking process with FA or with the same equilibrated protein for testing protein-protein interactions. A flexible docking approach performed with Haddock2.4 local version was used, as the protonation state of the ligand and of the protein had to be monitored. For the treatment of FA at different pH conditions, the protonation state was taken as reported in the literature (Poe, 1977; Szakacs & Noszál, 2006), while coordinates files were prepared using PRODRG (Schüttelkopf & van Aalten, 2004). The topology and parameter files used for the docking were obtained with the Automated Topology Builder (Malde et al., 2011), and ambiguous interaction restraints were defined according to the Haddock web server recommandations. Next, for holo-structures, the ANTECHAMBER module of AMBER18 using the General Amber Force Field (Wang, Wolf, Caldwell, Kollman & Case, 2004) was used for generating the parameter files for the FA in both protonation states. The best cluster for each pH according to Haddock grading score was then modeled and solvated in the same conditions as for the apo-protein, adapting the number of counterions and TIP3P water molecules added. All systems were subject MDS production using AMBER 18 package of programs, following the protocol described in the previous section.

2.5. *FA bioaccessibility assessment after in vitro digestion*

Both, WPI-FA and βlg-FA complexed systems and the respective controls, prepared at a concentration of 0.01825 g of dissolved species/100 g of solution, were subjected to a simulated gastrointestinal digestion (oral, gastric and intestinal phases). The procedure proposed by Minekus et al. (2014) was followed. After the *in vitro* digestion, samples were centrifuged at 4,500*g* for 10 min, and the obtained supernatants were collected. FA was quantified by the official AOAC microbiological method according to Corfield et al. (2020).

2.6. *Statistical analyses*

The results were expressed as the average of three replicates ± the standard deviation. The results obtained from different samples were compared with an ANOVA or T-Test analysis, as necessary, using the program GraphPad Prism 6.0.

3. Results and Discussion

3.1. ζ potential

In order to understand the occurrence and type of interactions, between βlg or WPI with FA, the ζ potential was analyzed. **Figure 1** shows the ζ potential for each single studied protein, βlg, or WPI, and for the corresponding mixed systems (βlg-FA, WPI-FA) at different concentrations at pH 3.0. The ζ potential, also termed as electrokinetic potential, is the potential at the slipping/shear plane of a colloid particle moving under an electric field (Kaszuba, Corbett, Mcneil-Watson & Jones, 2010). This parameter reflects the potential difference between the electric double layer of electrophoretically mobile particles and the layer of dispersant around them at the slipping plane. One of the most popular uses of ζ potential data is to relate it with colloid stability, in fact it was considered an indicator to predict and control the stability of colloidal suspensions. It can be noted that the response of any protein system is strongly dependent on its intrinsic structure and the charge modification induced by FA. The union between these milk proteins and FA probably induced subtle conformational changes in the protein molecule, i.e. subtle modifications in electrophoretic mobility and consequently in the ζ potential derived values.

ζ potential values for both proteins were in the order of the values previously reported by other authors. In this context, Haug, Skar, Vegarud, Langsrud & Draget (2009) reported that βlg presented a ζ potential close to 20 mV when it was at a pH below its isoelectric point (4.5), and Hu et al. (2020) indicated that WPI presented a ζ potential of approx. 25.7 mV in aqueous solution at pH 3.5. These results could be explained considering that the amino groups of the proteins would be positively charged, while the carboxyl groups would be in a neutral state (Chanamai & McClements, 2002; Haug, Skar, Vegarud, Langsrud & Draget, 2009) when the pH solutions were acidic.

Regarding the protein-FA systems, the ζ potential values were higher than those obtained for the single proteins, which could translate into greater colloidal stability. This result was similar to that obtained by Pérez et al. (2014), who found that βlg-FA mixed systems containing at 0.2% of proteins at pH 3.0 presented a ζ potential higher than that obtained for the control protein. These authors concluded that the interactions that governed these mixed systems were mainly of hydrophobic type. Binding FA to βlg is likely to induce conformational changes and may expose other charged areas to the protein surface, thus changing its electrophoretic

mobility and consequently the derived ζ potential values determined through DLS. measurement. In other terms, the hydrophobic pockets or patches of proteins would be blocked by the vitamin. In the global surface molecular features, the surface hydrophobicity would decrease and the electrokinetic potential would increase, i.e. higher ζ potential. Such an effect was less evident for WPI in comparison to βlg as can be noted in **Figure 1**. On the other hand, this behavior was different from that observed in a previous study by Corfield et al. (2020), in which protein-FA complexes prepared under similar conditions, but at much higher concentration (10% w/w) showed a ζ potential close to zero, suggesting that the interactions between proteins and FA were governed by electrostatic binding.

3.2. *Surface hydrophobicity (S_0)*

To analyze S_0 for the protein controls as well as for the complexes, the fluorescent probe 8-anilino-1-naphthalenesulfonic acid (ANS) was used due to its high intensity in hydrophobic environments (Ota, Tanaka & Takano, 2021). In all samples, it was observed that the maximum emission wavelength in the presence of the ANS probe was at 480 nm, demonstrating the presence of hydrophobic groups on the surface of the constituent proteins (Cardamone et. al., 1992). **Figure 2** shows the results obtained, observing that the S_0 of the WPI resulted higher than that obtained for its respective complexes. This implies that the proteins presented hydrophobic binding sites where the ANS probe could interact, i.e. ANS could interact with the complexes (Gasymov & Glasgow, 2007). Collin et al. (2003) studied the interaction between the βlg and the ANS fluorescent probe, and found that the protein had two binding sites, one internal and one external. By adding fatty acids to the βlg solution, they observed that the probe was mostly displaced to the internal site. Uhrinová et al. (2000) and Li et al. (2022b), explain that the internal hydrophobic cavity of βlg is controlled by the Tanford transition that involves the protonation/deprotonation of Glu89. Consequently, at neutral pH the protein is mostly open allowing the entry of other compounds, but at acidic pH the protein presents a closed conformation. In this sense, the binding of the ANS probe to βlg or WPI may ocurre in their external hydrophobic site, provided that the internal one is involved in FA binding at the low pH used in our experiments. In fact, the complexation process was carried out at pH 7.0 and the pH was subsequently adjusted to 3.0. It could be thought that at pH 7.0 the vitamin was able to bind to both, the internal and external hydrophobic sites, and then, by changing the conformation of the protein due to the pH decrease, the vitamin that interacted with the internal site could have been trapped, while the rest could interact with the external protein sites. Taking this hypothesis into account, when analyzing the S_0 corresponding to the complexes at pH 3.0,

the ANS would be competing against the vitamin only for the external hydrophobic sites. The decrease in S_0 of 78% for βlg-FA and 80% for WPI-FA compared to the control proteins shows that the vitamin presented greater affinity than the ANS probe for these hydrophobic sites.

3.3. *Kinetics of aggregation*

The optical density at 600 nm (OD 600) was analyzed to determine the aggregation process between proteins and FA to form complexes at pH 3.0. In all the cases studied, the changes in absorbance can be attributed to dispersion due to turbidity (Stirpe et al., 2011). **Figure 3** shows the aggregation curves obtained for the single vitamin (FA) and for the βlg-FA and WPI-FA mixed systems. All systems were evaluated at three different concentrations (0.00625%; 0.0125% and 0.01825%), at pH 3.0 and at 25°C. The proteins (βlg and WPI) did not show an increase of OD by their own during the kinetic study. According to the reports of Uhrinová et al. (2000), βlg at pH 2.6 showed more monomeric than dimeric forms as determined by nuclear magnetic resonance spectroscopy. These results could be due to the fact that at acidic pH far from pI, the protein tends to dissociate due to greater electrostatic repulsion. In addition, this protein presents its maximum self-association point (oligomer formation) and aggregation at the pH that coincides with the pI (4.8 – 5.0) (Uhrínová et al., 2000; Huag, Skar, Vegarud, Langsrud & Draget, 2009; Martínez & Pilosof, 2018). Contrary, the control of single FA presented a sizable increase in OD after one minute (**Figure 3a**). This could be explained considering the reports of Younis, Stamatakis, Callery & Meyer-stout (2009), who found that, under acidic medium, the electrostatic repulsions between the FA molecules are reduced, producing the vitamin self-association and later, the formation of polymorphic liquid crystals through molecular self-assembly with a columnar structure. There were differences between the OD–time curves for different concentrations of FA, which could be due to an effect of the concentration on the tendency towards molecular self-association of FA. In this sense, it seems that at a lower concentration, the FA has a greater facility to organize and form polymorphic liquid crystals.

Regarding the mixed systems, **Figures 3b** and **3c** show the curves obtained for the βlg-FA and WPI-FA complexes, respectively. Inset plots display the aggregation trend at short times. Both mixed systems showed similar behavior for the highest concentrations (0.0125% and 0.01825%), but different for the lowest concentration (0.00625%). In the case of βlg-FA at 0.00625%, a fast aggregation was observed compared to the higher concentrations of βlg-FA

systems, where the influence of FA was remarkable. On the contrary, the 0.00625% WPI-FA system showed a curve with a lower slope than the highest concentration of WPI-FA systems, showing that in this case the aggregation process was slower. These mixed systems manifested the influence of the respective proteins in the global behavior, i.e. proteins did not show OD increase by their own. When comparing the rates of formation of the aggregates (parameter K obtained from the non-linear fit) (**Table 1**), the differences between the formation of the complexes and the natural aggregation of FA at pH 3.0 are evident. In the case of the βlg-FA and WPI-FA complexes, the parameter K resulted lower in all cases compared to those obtained for the single FA systems. In other words, the formation process of protein-FA complexes was slower than the formation of FA crystals. This can be explained considering that the process of protein aggregate formation is complex since intermediates are generated that cooperate for the formation of the final product (Prudkin-Silva et al., 2018). In this sense, Tavares et al. (2015) studied the formation of complexes between FA and lactoferrin and showed that the mechanism of aggregate formation between these two species occurred in two steps: first, the FA molecules bind to the protein until it is saturated, and later, these reactive complexes self-associate and form aggregates a similar behavior as crystals nucleation and growth. This mechanism could also explain the formation of the βlg-FA and WPI-FA complexes.

3.4.*Molecular dynamics simulations (MDS)*

Aggregation kinetics results suggest that protein-FA co-precipitation at low pH derives from complex formation followed by self-association of those complexes. Protein-FA complexes were hence investigated through MDS, using βlg as a representative example of whey protein aggregation. Four binding site regions on βlg have been theoretically described in the literature: [a] the internal cavity of the β-barrel, [b] the outer surface near Trp19-Arg124, [c] the surface hydrophobic pocket in a groove between the α-helix and the β-barrel and [d] the aperture of the β-barrel (Roufik, Gauthier, Leng & Turgeon, 2006). Liang & Subirade (2010, 2012) have speculated after fluorescence experiments that the FA binding site on βlg at pH 7.0 is in a groove between the α-helix and the β-barrel (probably corresponding to site [c]). To determine the FA binding sites, we performed flexible docking of FA on a previously equilibrated protein. The 3 top-ranked binding sites obtained at pH 7.0 are shown in **Figure 4A**.

The highest-ranked complex structure shows a 300 ns-stable FA binding site at the aperture of the β-barrel (site [d]), in a position close to the retinol binding site described by Sawyer et al. (1998) and the quercetin binding site described by Mohseni-Shahri (2019). The time evolution

of the βlg-FA interactions within the 1-ligand complex at pH 7.0 (**Figure 3-SM**) highlights the stability of hydrophobic and electrostatic interactions in this binding site. Nonetheless, the results of Liang & Subirade (2010) fluorescence experiments showed no interference of retinol in FA-induced βlg fluorescence quenching in presence of molecules at pH 7.4. We thus started to investigate the second-best binding site located near the C-terminal of the protein, near Tyr42 and Tyr20. This binding site shows great stability during our simulation timescale (**Figure 3-SM**), through close polar contacts with unprotonated Glu157. The presence of this site could explain the greater quenching effect observed at $\lambda_{max} = \lambda_{TYR} = 280$nm in fluorescence experiments (Liang & Subirade, 2012), though it does not explain the relative fluorescence quenching observed at $\lambda_{max} = \lambda_{TRP} = 295$ nm, as FA remains far from any Trp residue if located in that binding site. The third best binding site is located near the groove between the α-helix and the β-barrel (site [c]), near Tyr102. This site is close to the one described by Liang & Subirade (2012): strong interaction with Tyr102 and Tyr99 and relative contact with Trp19 explains the quenching effect at both wavelengths. Nonetheless, **Figure 3-SM** shows the great vicinity of Arg124 to the ligand, suggesting a hybrid binding site between the groove and the outer surface binding site near Arg124-Trp19 (site [b]). This site is less stable than the two top-ranked, as illustrated by **Figure 3-SM** and **Figure 6**: the interaction distances remain above 4 Å and there is a high peak in the RMSF for the ligand, which suggests great instability for this FA binding site.

When the pH is lowered a so-called Tanford transition occurs and the β-barrel becomes less accessible (Ragona et al., 2003; Tian et al., 2006). This transition changes the electrostatic forces, inducing a significant environmental change in the interface between the α-helix and the β-barrel (Fogolari et al., 1998; 2000). The structural comparison for the apo-protein (**Table 2**) shows a decrease in the percentage of α-helix and β-sheet, but also an increase in the Non-polar/Polar SASA ratio suggesting a greater tendency for precipitation at lower pH.

Docking at pH 3.0 predicted at least 3 binding sites. The top-ranked binding site resides in the internal cavity of the calix (site [a]). In the hydrophobic pocket, FA interacts with mainly apolar residues of the internal cavity (Val41, Leu39, Met24) through both H-bonds and hydrophobic interactions, while FA's polar tail forms H-bonds with polar residues of the aperture of the barrel (Lys69, protonated Asp85). The presence of both types of interactions in FA binding to βlg had already been suggested in the literature (Liang & Subirade, 2012; Pérez et al., 2014). Nonetheless, this site has been described to preferentially bind fatty acids (Tian et al., 2006). Moreover, it was to be closed at low pH by the rotation of the E-F loop after the Tanford

412 transition of βlg (De Wit, 2009). Meanwhile, APBS calculations (**Figure 5**) show a diffusion
413 of the electrostatic repulsion at the entrance of the hydrophobic calix at pH 3.0; FA binding in
414 the internal cavity, perhaps less selective than at pH 7.0, may still be worth considering.

415 The second top-ranked binding site is located on the outer surface near Arg124-Trp19 (site [b]).
416 In site [b], we observed H-bond contacts with polar residues of a short helix (Gln13) or the end
417 of the β-barrel (Lys47) as observed in **Figure 4B** and **Figure 3-SM**. A third possible binding
418 location for FA on βlg at pH 3.0 is near the groove between the α-helix and the β-barrel (site
419 [c]). The interactions in site [c] are both hydrophobic and electrostatic. The pH-dependent
420 fluorescence quenching at $\lambda_{max} = \lambda_{TYR} = 295$nm observed by Liang & Subirade (2012), directly
421 linked with the instability and the lower number and strength of the contacts in site [c]
422 compared to pH 7.0 (**Figure 4A**), could be explained by the protonation of residues Glu157,
423 Glu131, Glu127 and Asp130 implicated in the βlg/FA interaction. Indeed, these last two
424 binding sites show great instability compared to their equivalents at pH 7.0, as shown by **Figure**
425 **3-SM** and **Figure 5**: we observe high amplitude oscillations in βlg-FA interactions distances
426 and a high peak in the RMSF of residue 163 (ligand).

427 In **Table 2**, the global ΔSASA (pH 3.0/pH 7.0) values obtained for apo and holo-structures (1
428 ligand) are reported. In order to best fit the aggregation kinetics observations (βlg, soluble at
429 pH 7.0, precipitates at pH 3.0 in the presence of FA), the most probable structures in the mix
430 should be the βlg-FA complexes showing the highest value of solvent accessible non-polar
431 surface (hydrophobic oligomerization) and the lowest value of polar surface (no solvent
432 screening) at pH 3.0, and vice versa at pH 7.0. As observed in the table, the difference of non-
433 polar/polar ratio between both pH decreases as a new ligand occupies a binding site. The
434 properties of the apo-structure could therefore most accurately fit the experimental
435 observations. Furthermore, $\Delta\Delta G_{MM\text{-}GBSA}$ (pH 3.0-pH 7.0) values reported in the table show that
436 the binding of one FA molecule at pH 3.0 is less favorable than at pH 7.0. This result seems
437 coherent with the predictions of Pérez et al. (2014) on the decrease in βlg-FA interactions at
438 low pH.

439 The afore mentioned results suggest that the unbound form of the protein was
440 thermodynamically preferred at pH 3.0. In order to explain the precipitation observed
441 experimentally, we thus chose to focus on the apo-dimer structure of βlg at acidic pH.

442 The top-ranked docking structure resulted in a symmetric dimer form at pH 3.0, but the
443 structure was unstable after a 30 ns MDS (as detailed by the time evolution of native contacts,

Figure 4-SM). This result, already reported in the literature (Uhrinová et al, 2000; Mercadante, 2010; Martínez & Pilosof, 2018) is in agreement with the stability of the OD for βlg observed during aggregation kinetics experiments, indicating a clear preference for the monomeric form in solution.

Interestingly, docking results for the dimer in the 1-ligand-bound state at pH 3.0 and subsequent 300 ns MDS yielded a perfectly stable structure for the whole simulated timescale. The structure is very similar to the one given by apo-dimer docking before equilibration and dissociation of the dimer. In terms of protein-ligand contacts within the holo-dimer (**Figure 6, Figure 4-SM**), the same region of amino-acids is implicated, and similar types of interactions are observed in for the two FA molecules (hydrophobic/H-bonds with apolar Val41/Leu39, H-bonds with polar Lys69/Asp85). Strong interactions between the two monomers in the β-sheets region, already suggested in the literature for symmetric apo-dimer formation at pH 7.0 (De Wit, 2009; Mercadante et al., 2010), are also reported here.

A SASA analysis focused on the residues implicated in dimer interaction as well as the representation of the solvent accessible surface difference between apo and holo-structures at both pH derived from APBS calculations are shown in **Figure 7**. We observe an important decrease in polar SASA between the apo- and holo-protein at pH 3.0, while at pH 7.0 the polar SASA increases. The charge repulsion in the region of Arg148 and in the α-helixes that prevents dimer formation according to Mercadante et al. (2010) is thus reduced upon ligand binding at pH 3.0, while it augments at pH 7.0. There is also a greater decrease in the non-polar SASA of these same residues upon ligand binding at pH 7.0 compared to pH 3.0. Both results suggest that a FA/βlg mix is more inclined to dimerization at acidic pH than a pure βlg solution. Nonetheless, this solely effect cannot explain the oligomerization and precipitation tendency of FA/βlg complexes at pH 3.0. Even though complex, these phenomena could be rationalized by a study of the holo-dimer solvent accessible surface (**Table 3**).

The non-polar/polar SASA ratio is greater for the complex1lig-complex1lig association at pH 3.0 than for the same association at pH 7.0 or for the apo-dimer at pH 7.0: holo-dimer at pH 3.0 could act as better aggregation nuclei than its counterparts. This would explain FA-βlg co-precipitation at pH 3.0 macroscopically visible at high protein concentrations (Corfield et al, 2020), while the apo-dimer and alo-dimer at neutral pH, showing a lower non-polar/polar SASA ratio, would remain soluble. In order to further investigate βlg-FA agglomeration at

acidic pH and to enlarge our study to more complex whey proteins, the next step was to characterize the co-precipitate itself.

3.5. *Particle size distribution*

Particle size distributions were evaluated in terms of volume (%), and number (%) for the proteins (βlg and WPI) and their respective mixed systems (βlg-FA and WPI-FA) prepared at three different concentrations at pH 3.0. The results obtained for the βlg protein solutions at pH 3.0 (**Figure 8**) showed that the distributions for the three concentrations were monomodal, showing one single peak which fell between the limits of 2.0 and 8.5 nm for the concentrations of 0.00625% and 0.0125% and between 3.0 and 11.6 for the 0.01825% system. This is coherent with our MDS showing that βlg at pH 3.0 is predominantly present as a monomer, but when concentrations vary, the hydrodynamic diameter can be modified (Martínez & Pilosof, 2018). On the other hand, the results of the WPI solutions at pH 3.0 showed that the distributions were bimodal, showing broad peaks at all the studied concentrations. These results are consistent with the composition of WPI, because the dehydration process used to obtain it can generate the partial aggregation of its protein components (Dissanayake, Kelly & Vasiljevic, 2010; Nishanthi, Chandrapala & Vasiljevic, 2017; Corfield et al., 2020).

Regarding the βlg-FA mixed systems, a polymodal distribution was observed, with hydrodynamic diameters shifted to higher values than those of the pure protein which are the result of the diversity of molecular interaction between the protein and FA components described above. There were mainly three to four peaks in the range between 25nm and 1500nm. These results coincide with those reported by Pérez et al. (2014), who observed that when FA was added to βlg solutions at pH 7.0, the particle sizes doubled.

With respect to the WPI-FA complexes (**Figure 9**), an effect similar to that obtained for βlg-FA was observed, since in all cases the complexes showed a displacement for the distributions to larger sizes. In the WPI-FA 0.00625% system, both in % volume and in number, two populations were observed in the range of 37 and 713 nm. On the other hand, in the WPI-FA systems with higher concentrations (0.0125% and 0.01825%), the populations were trimodal. The similarities between βlg and WPI in these particle size populations displacements suggests that WPI-FA interactions could be close to the ones described earlier for βlg, a WPI-FA holo-structure acting as aggregation nuclei for the co-precipitation.

When the polydispersity index was analyzed, for both protein and its respective mixed system, no significant change was detected as a consequence of complexation process (**Table 1-SM**).

3.6. Bioaccessibility of FA upon in vitro digestion

Given that protein-FA systems could be used as a strategy for FA carrier design and the vitamin delivery, it is relevant to evaluate its bioaccessibility after the gastrointestinal digestion. According Shahidi & Peng (2018), bioaccessibility is the percentage of the amount of a constituent released in the intestinal tract with respect to its total content. Bearing this concept in mind, the bioaccessible FA was evaluated by means of the official microbiological method, using *Lacticaseibacillus casei* BL23 (*L. casei* BL23) (auxotrophic strain for FA), after performing an *in vitro* digestion procedure for both, βlg-FA and WPI-FA mixed systems, and for the corresponding control systems (βlg, WPI, and FA). **Figure 10** shows the concentration of FA measured after the *in vitro* digestion process of the different systems prepared at a concentration of 0.01825%.

First, both the control system (FA) and the mixed systems (βlg-FA and WPI-FA) could be quantified by the *L. casei* BL23 model after subjecting them to an *in vitro* digestion, which implies that in the three systems the vitamin was bioaccessible. The results of the protein controls without FA showed that there was no microbial growth, confirming the validity of the experimental system (auxotrophy for the strain with respect to FA)

On the other hand, when comparing the mixed systems with the control, the FA concentration obtained for βlg-FA system did not show significant differences. However, in the case of WPI-FA system, higher FA concentration values were observed with respect to the free FA. This behavior could suggest that the vitamin within the WPI-FA system was more stable or more resistant when submitted to the *in vitro* digestion treatment compared to that present in the βlg-FA system or the free FA. Shakoor, Pamunuwa & Karunaratne (2022) found that the bioaccessibility of FA in a system made up of chickpea protein was lower than that obtained in a system made up of alginate-FA, because the chickpea protein was affected by pepsin in the gastric stage of *in vitro* digestion, promoting the release of the vitamin. In the case of βlg-FA, being a simpler system than WPI-FA, made up of a single protein, it could be affected in the same way as chickpea proteins. In this sense, βlg is of great relevance to study milk protein-FA complexes in a more simplified way, however, it should be noted that the complexity of the WPI constitution provides greater protection to the vitamin. Even when comparing the results

obtained by Shakoor, Pamunuwa & Karunaratne (2022) in their best system (alginate-FA), WPI-FA showed 12% more bioaccessibility of FA. These results suggest that the mixed systems could be considered appropriate for FA delivery. Experiments are being carried out to determine the bioavailability of FA in human cell culture models, such as transcytosis systems.

4. Conclusions

Whey protein and folic acid interactions were proven highly pH-dependent. The *in vitro* studies allowed to characterize the constituted complexes size, suggesting that in these systems, the interactions between the proteins and the FA are mainly hydrophobic. A model holostructure for the βlg dimer at pH 3.0 arose as possible aggregation nuclei to explain co-precipitation at acidic pH. The new insights we provide on this key step of protein-FA complex formation could help the development of drug delivery systems or potential food ingredients. The results of bioaccesibility show that the best option would be the WPI-FA system, as it allows getting higher concentration of bioaccessible vitamin. Although both proteins have potential for complexes development, WPI also has the advantage of being a cheaper protein source. Complexes here described could be used as ingredients to be incorporated into foods consumed by people with special diets such as pregnant women.

5. Acknowledgements

The present report was supported by grants from the ANPCyT (PICT 2017-1683), UBACyT 20020150100079BA, UBACyT 20020190200136BA and PIP 112202101 00072CO Consejo Nacional de Investigaciones Científicas y Técnicas (CONICET). We acknowledge computational resources granted by the Facultad de Ciencias Exactas y Naturales, Universidad de Buenos Aires (cluster CECAR). SDL, OEP, MCA, KM and CCS are members of the research career of the Argentinian National Research Council CONICET. Authors thanks to Laboratorios Bagó of Argentina for folic acid and ARLA Food for WPI donation, respectively.

6. Conflict of interest

The authors declare no conflict of interest.

7. References

Al-Jassar, S. A.; Mikajiri, S.; Roos, Y. J. (2020). Rehydration of whey protein isolate: Effect of temperature, water activity, and storage time. LWT-Food Science and Technology, 133:110099. https://doi.org/10.1016/j.lwt.2020.110099.

Assanelli, D.; Bonanome, A.; Pezzini, A.; Albertini, F.; Maccalli, P.; Grassi, M.; … Visioli, F. (2004). Folic acid and Vitamin E supplementation effects on homocysteinemia, endothelial function

and plasma antioxidant capacity in young myocardial-infarction patients. Pharmacological Research, 49(1):79–84. https://doi.org/10.1016/j.phrs.2003.07.009.

Bashford, D.; Karplus, M. (1990). pK_a´s of Ionizable Groups in Proteins: Atomic Detail from a Continuum Electrostatic Model. Biochemistry, 29: 10219-10225. https://doi.org/10.1021/bi00496a010.

Carpineti, L.; Martínez, J.; Pilosof, A.; Pérez, O. (2014). β-Lactoglobulin–carboxymethylcellulose core–shell microparticles: Construction, characterization and isolation. Journal of Food Engineering, 131:65-74. https://doi.org/10.1016/j.jfoodeng.2014.01.018.

Carter, B. G.; Drake, M. A. (2018). Invited review: The effects of processing parameters on the flavor of whey protein ingredients. J. Dairy Sci. 101:6691–6702. https://doi.org/10.3168/jds.2018-14571.

Case, D. A.; Cheatham, T. E; Darden, T.; Gohlke, H.; Luo, R. Merz, K. M.; Onufriev, A.; Simmerling, C.; Wang, B.; Woods, R. J. (2005). The Amber biomolecular simulation programs. Journal of Computational Chemistry, 26 (16): 1668-1688. https://doi.org/10.1002/jcc.20290.

Case, D.A.; Belfon, K., Ben-Shalom, I.Y.; Brozell, S.R.; Cerutti, D.S.… Kollman, P.A. (2020), AMBER 2020, University of California, San Francisco.

Chanamai, R.; McClements, D. (2002). Comparison of gum arabic, modified starch, and wheyprotein isolate as emulsifiers: Influence of pH, $CaCl_2$ and temperature. Journal of Food Science, 67 (1):120-125. https://doi.org/10.1111/j.1365-2621.2002.tb11370.x.

Collini, M.; D´Alfonso, L.; Molinari, H.; Ragona, L.; Catalano, M.; Baldini, G. (2003). Competitive binding of fatty acids and the fluorescent probe 1-8-anilinonaphthalene sulfonate to bovine β-lactoglobulin. Protein Sci. 12(8): 1596–1603. https://doi: 10.1110/ps.0304403.

Corfield, R.; Martínez, K. D.; Allievi, M., C.; Santagapita, P.; Mazzobre, F.; Schebor, C.; Pérez, O. E. (2020). Whey proteins-folic acid complexes: Formation, isolation and bioavailability in a Lactobacillus casei model. Food Structure, 26:100162. https://doi.org/10.1016/j.foostr.2020.100162.

De Wit, J. (2009). Thermal behaviour of bovine β-lactoglobulin at temperatures up to 150°C. a review. *Trends in Food Science & Technology*, 20, 27-34. https://doi.org/10.1016/j.tifs.2008.09.012

De Wolf, F.A.; Brett, G. M. (2000). Ligand-binding proteins: Their potential for application in systems for controlled delivery and uptake of ligands. Pharmacological Reviews, 52(2), 207–236. https://pharmrev.aspetjournals.org/content/52/2/207.

Dissanayake, M.; Kelly, A.; Vasiljevic, T. (2010). Gelling Properties of Microparticulated Whey Proteins. J. Agric. Food Chem, 58:6825-6832. https://doi.org/10.1021/jf1009796.

606 Dolinsky, J. T.; Nielsen, J. E.; McCammon, J. A.; Baker, N.A. (2004). PDB2PQR: an automated
607 pipeline for the setup, execution, and analysis of Poisson-Boltzmann electrostatics calculations.
608 *Nucleic Acid Research*, 32: 665-667. https://doi.org/10.1093/nar/gkh381.

609 Eudes, A., Erkens, G. B., Slotboom, D. J., Rodionov, D. A., Naponelli, V., & Hanson, A. D. (2008).
610 Identification of genes encoding the folate- and thiamine-binding membrane proteins in
611 firmicutes. Journal of Bacteriology, 190(22), 7591–7594. https://doi.org/10.1128/JB.01070-08.

612 FAO; WHO. (2004). Vitamin and mineral requirements in human nutrition. Second edition. World
613 Health Organization and Food and Agriculture Organization of the United Nations, 1–362.
614 https://doi.org/92 4 154612 3.

615 Farooq, M. A.; Aquib, M. D.; Ghayas, S.; Bushra, R.; Khan, D. H.;Parveen, A.; Wang, B. (2019). Whey
616 protein: A functional and promising material for drug delivery systems recent developments
617 and future prospects. Polym Adv Technol. 30:2183–2191. https://doi.org/10.1002/pat.4676.

618 Fogolari F.; Ragona L.; Zetta L.; Romagnoli S.; De Kruif K.G.; Molinari H. (1998). Monomeric bovine
619 b-lactoglobulin adopts a-barrel fold at pH 2. FEBS Letters, 436: 149-154.
620 https://doi.org/10.1016/S0014-5793(98)00936-3

621 Fogolari F.; Ragona L.; Licciardi S.; Romagnoli S.; Michelutti R.; Ugolini R. (2000). Electrostatic
622 properties of bovine beta-lactoglobulin**.** Proteins: Structure, Function, and Genetics, 39: 317-
623 330. https://doi.org/10.1002/(SICI)1097-0134(20000601)39:4<317::AID-PROT50>3.0.CO;2-
624 W

625 Frommherz, L.; Martiniak, Y.;Heuer, T.; Roth, A.; Kulling, S. E.; Hoffmann, I. (2014). Degradation of
626 folic acid in fortified vitamin juices during long term storage. Food chemistry, 159, 122–127.
627 https://doi.org/10.1016/j.foodchem.2014.02.156.

628 Gasymov, O. K.; Glasgow, B. J. (2007). ANS fluorescence: Potential to augment the identification of
629 the external binding sites of proteins. Biochimica et Biophysica Acta, 1774, 403–411.
630 https://doi.org/10.1016/j.bbapap.2007.01.002.

631 Gazzali, A. M.; Lobry, M.; Colombeau, L.; Acherar, S.; Azaïs, H.; Mordon, S.; Arnoux, P.; Baros, F.;
632 Vanderesse, R.; Frochot, C. (2016). Stability of folic acid under several parameters. European
633 Journal of Pharmaceutical Sciences, 93, 419-430.

634 Genheden S, Ryde U. The MM/PBSA and MM/GBSA methods to estimate ligand-binding affinities.
635 Expert Opin Drug Discov. 2015 May;10(5):449-61. https://doi.org/
636 10.1517/17460441.2015.1032936.

637 Halabi, A.; Deglaire, A.; Hamon, P.; Bouhallab, S.; Dupont, D.; Croguennec, T. (2020). Kinetics of
638 heat-induced denaturation of proteins in model infant milk formulas as a function of whey

protein composition. Food Chemistry, 302:125296. https://doi.org/10.1016/j.foodchem.2019.125296.

Henderson, G. B., Zevely, E. M., & Huennekens, F. M. (1979). Coupling of energy to folate transport in *Lactobacillus casei*. Journal of Bacteriology, 139(2), 552–559. https://doi.org/10.1128/jb.139.2.552-559.1979.

Hu, Y.; He, C.; Jiang, C.; Liao, Y.; Xiong, H.; Zhao, Q. (2020) Complexation with whey protein fibrils and chitosan: A potential vehicle for curcumin with improved aqueous dispersion stability and enhanced antioxidant activity. Food Hydrocolloids, 104:1-10. https://doi.org/10.1016/j.foodhyd.2020.105729.

Haug, I. J.; Skar, H. M.; Vegarud, G. E.; Langsrud, T.; Draget, K. I. (2009). Electrostatic effects on β-lactoglobulin transitions during heat denaturation as studied by differential scanning calorimetry. Food Hydrocolloids, 23:2287–2293. https://doi.org/10.1016/j.foodhyd.2009.06.006,

Jorgensen, W.L.; Chandrasekhar, J.; Madura, J.D.; Impey, R.W.; and Klein, M.L. (1983). Comparison of simple potential functions for simulating liquid water. J. Chem. Phys. 79: 926–935. https://doi.org/10.1063/1.445869

Kaszuba, M.; Corbett, J.; Mcneil-Watson, F.; Jones, A. (2010). High-concentration zeta potential measurements using light-scattering techniques. Phil. Trans. R. Soc. A. 368, 4439–4451. https://doi.org/10.1098/rsta.2010.0175.

Klose D. P.; Wallace B. A.; Janes R. W. (2010). 2Struc: the secondary structure server. Bioinformatics 26(20): 2624-2625. https://doi.org/10.1093/bioinformatics/btq480.

Kunji, E. R. S.; Mierau, I.; Hagting, A.; Poolman, B.; Konings, W. N. (1996). The proteolytic system of lactic acid bacteria. International Journal of General and Molecular Microbiology, 9(2), 90–106. https://pure.rug.nl/ws/portalfiles/portal/10265039/1996AntonievLeeuwenhoekKunji.pdf.

Li, H.; Robertson, A.D.; Jensen, J. H. (2005). Very Fast Empirical Prediction and Rationalization of Protein pKa Values. Proteins: Structure, Function, and Bioinformatics 61:704 –721. https://doig.org/10.1002/prot.20660.

Li, H.; Wang, T.; Hu, Y.; Wu, J.; Van der Meeren, P. (2022a). Designing delivery systems for functional ingredients by protein/ polysaccharide interactions. Trends in Food Science & Technology. 119: 272-287. https://doi.org/10.1016/j.tifs.2021.12.007.

Li, H.; Wang, T.; Su, J.; Van der Meer, P. (2022b). Influence of pH and low/high- methoxy pectin complexation on the hydrophobic binding sites of β-lactoglobulin studied by a fluorescent probe method. Food Hydrocolloids, 133, 108020. https://doi.org/10.1016/j.foodhyd.2022.108020.

672 Liang, L.; Subirade, M. (2012). Study of the acid and thermal stability of b-lactoglobulin–ligand
673 complexes using fluorescence quenching. Food Chem. 132: 2023-2029.
674 https://doi.org/10.1016/j.foodchem.2011.12.043.

675 Liang, L.; Subirade, M. (2010). β -Lactoglobulin/Folic Acid Complexes: Formation, Characterization,
676 and Biological Implication J. Phys. Chem. B., 114:6707-6712.
677 https://doi.org/10.1021/jp101096r.

678 Maier, J.A.; Martinez, C.; Kasavajhala, K.; Wickstrom, L.; Hauser, K.E.; and Simmerling, C. (2015).
679 ff14SB: improving the accuracy of protein side chain and backbone parameters from ff99SB. J.
680 Chem. Theor. Comput., 11: 3696–3713. https://doi.org/10.1021/acs.jctc.5b00255.

681 Makori, S. I. ; Mu, T.; Sun, H. (2021). Functionalization of sweet potato leaf polyphenols by
682 nanostructured composite β-lactoglobulin particles from molecular level complexations: A
683 review Food Chemistry, 372: 131304. https://doi.org/10.1016/j.foodchem.2021.131304.

684 Malde, A.K.; Zuo, L.; Breeze, M.; Stroet, M.; Poger, D.; Nair, P. C.; Oostenbrink, O.; Mark, A. E.
685 (2011). An Automated force field Topology Builder (ATB) and repository: Version 1.0. *J.*
686 *Chem. Theory Comput.*, 7(12): 4026-4037. https://doi.org/10.1021/ct200196m.

687 Martínez, J.H., Velázquez, F., Burrieza, H.P., Martínez, K.D., Paula Domínguez Rubio, A., dos Santos
688 Ferreira, C., Pérez, O.E., 2019. Betanin loaded nanocarriers based on quinoa seed 11S globulin.
689 Impact on the protein structure and antioxidant activity. Food Hydrocolloids 87, 880–890.
690 https://doi.org/10.1016/j.foodhyd.2018.09.016.

691 Martínez, J.; Pilosof, A. M. R. (2018). On the relationship between pH-dependent β- lactoglobulin self
692 assembly and gelation dynamics. International Food Research Journal, 25(2):676-683.
693 https://ri.conicet.gov.ar/handle/11336/92479.

694 Mercadante, D.; Melton, L. D.; Norris, G. H.; Loo, T. S.; Williams, M. A. K.; Dobson, R. C. J.; Jameson,
695 G. B. (2010). Bovine β -Lactoglobulin Is Dimeric Under Imitative Physiological Conditions:
696 Dissociation Equilibrium and Rate Constants over the pH Range of 2.5–7.5. Biophysical
697 Journal, 103(2). https://doi.org/10.1016/j.bpj.2012.05.041.

698 Minekus, M., Alminger, M., Alvito, P., Ballance, S., Bohn, T., Bourlieu, C., … Brodkorb, A. (2014). A
699 standardised static *in vitro* digestion method suitable for food-an international consensus. *Food*
700 *and Function*, *5*(6), 1113–1124. https://doi.org/10.1039/c3fo60702j.

701 Mohammed, A-L. Y.; Dyab, A.K. F.; Taha, F.; Abd-El-Mageed, A.I. A. (2021). Encapsulation of folic
702 acid (vitamin B9) into sporopollenin microcapsules: Physico-chemical characterisation, *in vitro*
703 controlled release and photoprotection study. Materials Science & Engineering C, 128:112271.
704 https://doi.org/10.1016/j.msec.2021.112271.

Mohseni-Shahri, S.F. (2019). Study of the Interaction of quercetin and taxifolin with β-Lactoglobulin by Fluorescence Spectroscopy and Molecular Dynamics Simulation. *Journal of Applied Spectroscopy*. 86 (1): 154-161. https://doi.org/10.1007/s10812-019-00796-3.

Neves, D. A.; Brito de Sousa-Lobato, K.; Simões-Angelica, R.; Teixeira Filho, J.; Pisanelli-Rodrigues de Oliveira, G.; Teixeira Godoy, H. (2019). Thermal and *in vitro* digestion stability of folic acid in bread. Journal of Food Composition and Analysis, 84: 103311. https://doi.org/10.1016/j.jfca.2019.103311.

Nishanthi, M.; Chandrapala, J.; Vasiljevic, T. (2017). Compositional and structural properties of whey proteins of sweet, acid and salty whey concentrates and their respective spray dried powders. International Dairy Journal, 74:49-56. https://doi.org/10.1016/j.idairyj.2017.01.002.

Ochnio, M. E.; Martínez, J. H.; Allievi, M. C.; Palavecino, M.; Martínez, K. D.; Pérez, O. E. (2018). Proteins as nano-carriers for bioactive compounds. The case of 7S and 11S soy globulins and folic acid complexation. Polymers, 10(2), 1–21. https://doi.org/10.3390/polym10020149.

Ota, C.; Tanaka, S.; Takano, K. (2021). Revisiting the Rate-Limiting Step of the ANS–Protein Binding at the Protein Surface and Inside the Hydrophobic Cavity. Molecules, 26(2) 420. https://doi.org/10.3390/molecules26020420.

Pangallo, D.; Kraková, L.; Puškárová, A.; Šoltys, K.; Bučková, M.; Koreňová, J.; … Kuchta, T. (2019). Transcription activity of lactic acid bacterial proteolysis-related genes during cheese maturation. Food Microbiology, 82, 416–425. https://doi.org/10.1016/j.fm.2019.03.015.

Paul, B. K.; Ghosh, N.; Mukherjee, S. (2014). Binding interaction of a prospective chemotherapeutic antibacterial drug with β-lactoglobulin: Results and challenges. Langmuir the ACS Journal of Surfaces and Colloids, 30(20), 5921–5929. https://doi.org/10.1021/la501252x.

Pérez, A.; Andermatten R.; Rubiolo, A.; Santiago, L. (2014) β-Lactoglobulin heat-induced aggregates as carriers of polyunsaturated fatty acids. Food Chemistry, 158, 66-72. https://doi.org/10.1016/j.foodchem.2014.02.073.

Pérez, O.E.; David-Birman, T.; Kesselman, E.; Levi-Tal, S.; Lesmes, U. (2014). Milk protein e vitamin interactions: Formation of beta-lactoglobulin/folic acid nano-complexes and their impact on *in vitro* gastro-duodenal proteolysis. Food Hydrocolloids, 38: 40–47. https://doi.org/10.1016/j.foodhyd.2013.11.010.

Poe, M. (1977). Acidic dissociation constants acid, and methotrexate of folk acid, dihydrofolic. The Journal of Biological Chemistry, 252 (11), 3724–3729. Retrieved from http: https://www.jbc.org/article/S0021-9258(17)40312-7/pdf.

Prudkin-Silva, C.; Martínez, J. H.; Martínez, K. D.; Farías, M. E.; Coluccio-Leskow, F.; Pérez, O. E. (2018). Proposed molecular model for electrostatic interactions between insulin and chitosan. Nano-complexation and activity in cultured cells. Colloids and Surfaces A, 537:425-434. http://dx.doi.org/10.1016/j.colsurfa.2017.10.040.

Qie, X.; Chen, W.; Zen, M.; Wang, Z.; Chen, J.; Goff, H.D.; He, Z. (2021). Interaction between β-lactoglobulin and chlorogenic acid and its effect on antioxidant activity and thermal stability. Food Hydrocolloids, 121: 107059, 1-12. https://doi.org/10.1016/j.foodhyd.2021.107059.

Ragona L.; Fogolari F.; Catalano M.; Ugolini R.; Zetta L.; Molinari H. (2003). EF loop conformational change triggers ligand binding in β-lactoglobulins. The Journal of Biological Chemistry, 278: 38840-38846. https://doi.org/10.1074/jbc.M306269200.

Roufik, S.; Gauthier, S. F.; Leng, X.; Turgeon, S. L, (2006). Thermodynamics of Binding Interactions between Bovine Beta-Lactoglobulin A and the Antihypertensive Peptide Beta-lg f142-148, Biomacromolecules**,** 7, 419-426. https://doi.org/10.1021/bm050229c.

Ruiz-Rico, M.; Pérez-Esteve, É.; Lerma-García, M.J.; Marcos. M.D.; Martínez-Máñez, R.; Barat, J.M. (2017). Protection of folic acid through encapsulation in mesoporous silica particles included in fruit juices. Food Chem. 218:471-478. https://doi.org/10.1016/j.foodchem.2016.09.097.

Ryckaert, J. P.; Ciccoti, G.; Berendsen, H. J. (1977). Numerical integration of the Cartesian Equations of Motion of a System with Constraints: Molecular Dynamics of n-Alkanes. *J. Comp. Phys*, 23(3):321-341. https://doi.org/10.1016/0021-9991(77)90098-5.

Savijoki, K.; Ingmer, H.; Varmanen, P. (2006). Proteolytic systems of lactic acid bacteria. Applied Microbiology and Biotechnology, 71(4), 394–406. https://doi.org/10.1007/s00253-006-0427-1.

Sawyer, L.; Brownlow, S.; Polikarpov, I.; Wu, S. Y. (1998). β-lactoglobulin: *Structural Studies Biological Clues*, 8(2), 0–72. https://doi.org/10.1016/S0958-6946(98)00021-1.

Scholl, T.; Johnson, W. (2000). Folic acid: influence on the outcome of pregnancy. Am J Clin Nutr, 71:1295-303. https://doi.org/10.1093/ajcn/71.5.1295s.

Scḧuttelkopf, A. W.; van Aalten, D. M. F.; PRODRG: a tool for high-throughput crystallography of protein-ligand complexes. Acta Crystallographica Section D, 60:1355–1363. https://doi.org/10.1107/S0907444904011679.

Sengupta, B.; Das, N.; Sen, P. (2018). Monomerization and aggregation of β-lactoglobulin under adverse condition: A fluorescence correlation spectroscopic investigation. BBA - Proteins and Proteomics 1866 (2018) 316–326. https://doi.org/10.1016/j.bbapap.2017.11.007.

Shao, J.; Tanner, S. W.; Thompson, N.; Cheatham, N. T. (2007). Clustering Molecular Dynamics Trajectories: Characterizing the Performance of Different Clustering Algorithms. J.Chem. Theory Comput., 3(6), 2312–2334. https://doi.org/10.1021/ct700119m.

Sindhikara, D.; Kim, S.; Voter, A.; Roitberg, A. E. (2009). Bad Seeds Sprout Perilous Dynamics: Stochastic Thermostat Induced Trajectory Synchronization in Biomolecules. *J. Chem. Theory Comput.*5 (6):1624–1631. https://doi.org/10.1021/ct800573m.

Štěpánek, P. (1993). Static and dynamic properties of multiple light scattering. The Journal of Chemical Physics, 99: 6384-6393. https://doi.org/10.1063/1.465877.

Stirpe, A.; Pantusa, M.; Rizzuti, B.; Sportelli, L.; Bartucci, R.; Guzzi, R. (2011). Early stage aggregation of human serum albumin in the presence of metal ions, International Journal of Biological Macromolecules 49 (2011) 337– 342. https://doi.org/10.1016/j.ijbiomac.2011.05.011.

Szakacs, Z.; Noszál, B. (2006). Determination of dissociation constants of folic acid, methotrexate, and other photolabile pteridines by pressure-assisted capillary electrophoresis**.** *Electrophoresis*, 27 (17): 3399-3409. https://doi.org/10.1002/elps.200600128.

Tang, C. (2021). Assembled milk protein nano-architectures as potential nanovehicles for nutraceuticals. Advances in Colloid and Interface Science, 219: 102432. https://doi.org/10.1016/j.cis.2021.102432.

Tavares, G. M.; Croguennec, T.; Lê, S.; Lerideau, O.; Hamon, P.; Carvalho, A. F.; Bouhallab, S. (2015). Binding of Folic Acid Induces Specific Self-Aggregation of Lactoferrin: Thermodynamic Characterization. Langmuir, 31: 12481−12488. https://doi.org/10.1021/acs.langmuir.5b02299.

Tian, F.; Johnson, K.; Lesar, A. E.; Moseley, H.; Ferguson, J.; Samuel, I. D. W.; Mazzini, A.; Brancaleon, L. (2006). The pH-dependent conformational transition of beta-lactoglobulin modulates the binding of protoporphyrin IX. Biochimica et Biophysica Acta, 1760: 38 – 46. https://doi.org/10.1016/j.bbagen.2005.09.005.

Uberuaga, B. (2004). Synchronization of trajectories in canonical molecular dynamics simulations: Observation, explanation, and exploitation. *J. Chem. Phys*, 20 (14): 6363-6374. https://doi.org/10.1063/1.1667473.

Uhrínová, S.; Smith, M. H.; Jameson, G. B.; Uhrín, D.; Sawyer, L.; Barlow, P. N. (2000). Structural changes accompanying pH-induced dissociation of the β-lactoglobulin dimer. Biochemistry, 39:3565-3574. https://doi.org/10.1021/bi992629o.

Wang, J.; Wolf, R. M.; Caldwell, J. W.; Kollman, P. A.; Case, D. A. (2004). Development and Testing of a General Amber Force Field. *J. Comp. Chem.*,25 (9): 1157-1174**.** https://doi.org/10.1002/jcc.20035.

801 Weiser, J.; Shenkin, P. S.; Still, W. C. (1999). Approximate solvent-accessible surface areas from
802 tetrahedrally directed neighbor densities. Biopolymers, 50 (4):373-380.
803 https://doi.org/10.1002/(SICI)1097-0282(19991005)50:4<373::AID-BIP3>3.0.CO;2-U.

804 Younis, I. R., Stamatakis, M. K., Callery, P. S., & Meyer-stout, P. J. (2009). Influence of pH on the
805 dissolution of folic acid supplements. International Journal of Pharmaceutics, 367, 97–102.
806 https://doi.org/10.1016/j.ijpharm.2008.09.028.

807 Zhang, J.; Liu, X.; Subirade, M.; Zhou, P.; Liang, L. (2014). A study of multi-ligand beta-lactoglobulin
808 complex formation. Food Chemistry 165: 256-261.
809 http://dx.doi.org/10.1016/j.foodchem.2014.05.109.

810 Zhang, S., Li, L., Ai, B., Zheng, L., Zheng, X., Yang, Y., Xiao, D., Sheng, Z. (2022a). Binding of β-
811 lactoglobulin to three phenolics improves the stability of phenolics studied by multispectral
812 analysis and molecular modeling. Food Chemistry: X, 15 10036.
813 https://doi.org/10.1016/j.fochx.2022.100369.

814 Zhang, X.; Lu, Y.; Zhao, R.; Wang, C.; Wang, C.; Zhang, T. (2022b). Study on simultaneous binding
815 of resveratrol and curcumin to β-lactoglobulin: Multi-spectroscopic, molecular docking and
816 molecular dynamics simulation approaches Food Hydrocolloids, 124, 107331.
817 https://doi.org/10.1016/j.foodhyd.2021.107331.

818

Table 1: K parameter determined by fitting the OD vs. time curves (**Eq. 1**)

Sample		K (min^{-1})	R^2
βlg-FA	0.00625	4.81 ± 0.50	0.92
	0.0125	0.44 ± 0.02	0.96
	0.01825	0.580 ± 0.03	0.95
WPI-FA	0.00625	0.292 ± 0.02	0.92
	0.0125	0.356 ± 0.02	0.94
	0.01825	0.674 ± 0.03	0.94
FA	0.00625	7.80 ± 3.30	0.92
	0.0125	1.71± 0.02	0.96
	0.01825	1.41 ± 0.08	0.95

Table 2: Characterization of the most probable structures after clusterization on a 300ns MDS. Non-polar and polar characterize the contribution of protein residues to the total SASA, while all atoms include the sum of both protein and ligand atoms. For details and graphical description, see Supplementary Materials **(1.1-SM)**.

Structures		Apo-βlg	Holo-βlg
$\Delta R_{radius\ of\ gyration}$(pH3-pH7)		-0.05 Å	0.01 Å
Secondary Structure Analysis*: Δ(pH3-pH7)	Helix	-3.0 %	0.7 %
	Sheet	-3.1 %	0.3 %
ΔSASA (pH3-pH7)	All atoms	-127.2	435.6
	Non polar	29	153.9
	Polar	-156.3	226.1
	Ligand(s)	/	37.0
	Non-polar/Polar ratio	0,06	-0.03
$\Delta\Delta H_{MM\text{-}GBSA}$(pH3-pH7)		/	11.2103 kcal/mol
$\Delta\Delta G_{MM\text{-}GBSA}$(pH3-pH7)		/	6.9 kcal/mol

*Data obtained through the DSSP Method (Klose et al, 2010)

Table 3: Characterization of the most probable dimer structures after clusterization on a 300 ns MDS. For details and graphical description, see Supplementary Materials **(1.1-SM)**. Non-polar and polar characterize protein residues contribution to the total SASA, while all atoms include the sum of both protein and ligand atoms.

Structures		Apo-dimer pH 7.0	Holo-dimer pH 7.0	Holo-dimer pH 3.0
SASA	All atoms	15704,6	15835,2	16092,1
	Non polar	8535,9	8061,5	8583,5
	Polar	7168,6	7024,9	7118,2
	Ligand(s)	/	173,82 (inner2) 318,44 (inner1)	177,57 (inner2) 212,87(inner1)
	Non-polar/Polar ratio	1,191	1,148	1,206

Figure captions

Figure 1: ζ potential of protein components in comparison with protein-FA mixed systems in three concentrations (1: 0.00625%; 2: 0.0125%; 3: 0.01825%), and pH 3.0. A) βlg and βlg-FA; B) WPI and WPI-FA. Different letters indicate significant differences $p \leq 0.05$. Lowercase letters correspond to the βlg system and uppercase letters to the WPI system.

Figure 2. Surface hydrophobicity (S_0) for βlg and WPI in comparison with S_0 for βlg-FA and WPI-FA mixed systems. Different letters indicate significant differences $p \leq 0.05$.

Figure 3. Time dependence of the OD at 600 nm normalized for A) FA; B) βlg-FA and C) WPI-FA, registered in three concentrations (0.00625% (red); 0.0125% (blue); 0.01825% (black)); pH 3.0 and 25°C. The solid lines correspond to the best fit according to **Eq. (1).** The insets show the behavior of OD600 at short time. Error bars are within the symbols.

Figure 4: A stereocartoon of the mainchain fold of the most probable protein apo-structure A) at pH 7.0, B) pH 3.0 obtained after docking and MD equilibration. The strands of β-sheet are shown as arrows and the helices as coils. Residues are colored by type: acid (red), basic (marine), polar (green) and apolar (white). The Tyr residues close to the ligand are colored in deep purple, Trp residues in pink. Polar contacts are represented by dotted yellow lines, and residues in contact with ligands are labeled.

Figure 5: A stereocartoon of the mainchain fold of the most probable protein apo-structure A) at pH 7.0, B) pH 3.0 obtained after docking, MD equilibration. The Adaptive Poisson-Boltzmann Solver (APBS) analysis (Dolinsky et al., 2004) was performed on both structures to obtain a representation of the solvent excluded surface (Connolly surface; min = -1kT/e, max = 1kt/e). The strands of β-sheet are shown as arrows and the helices as coils. Residues are colored by type: acid (red), basic (marine), polar (green) and apolar (white). Figure C) represents an alignment of βlg at pH 7.0 (green) and pH 3.0 (red), showing the rotation of the E-F loop. Yellow dots report unaligned atoms, contributing to a global RMSD of 0.79 A°.

Figure 6: A stereocartoon of the mainchain fold of the most probable protein apo-structure at pH 3.0 obtained after docking and MD equilibration. The strands of β-sheet are shown as arrows and the helices as coils. Residues are colored by type: acid (red), basic (marine), polar

868 (green) and apolar (white). Polar contacts are represented by dotted yellow lines, and residues
869 in contact with ligands are labeled.

870 **Figure 7**: Solvent Accessible Surface Area representation of apo (transparent surface) and holo
871 (solid surface)-monomers (min = -1kT/e, max = 1kt/e) at A) pH 7.0, B) pH 3.0. The ΔSASA
872 (holo-apo) values corresponding to the residues implicated in the dimer interaction are gathered
873 in the graph below each structure.

874 **Figure 8**: Particle size distribution of βlg protein solutions (dotted lines) and mixed βlg-FA
875 systems (red lines) prepared at pH 3.0 and evaluated at concentrations of0.00625 g/100g;
876 0.0125 g/100g and 0.0182 g/100g.

877 **Figure 9**: Particle size distribution of WPI protein solutions (dotted lines) and mixed WPI-FA
878 systems (blue lines) prepared at pH 3.0 and evaluated at concentrations of 0.00625 g/100g;
879 0.0125 g/100g and 0.0182 g/100g.

880 **Figure 10**: FA bioaccessibility after *in vitro* digestion. The systems concentration was
881 0.01825% (w/w). Different letters indicate significant differences $p \leq 0.05$.

882

883

884

885

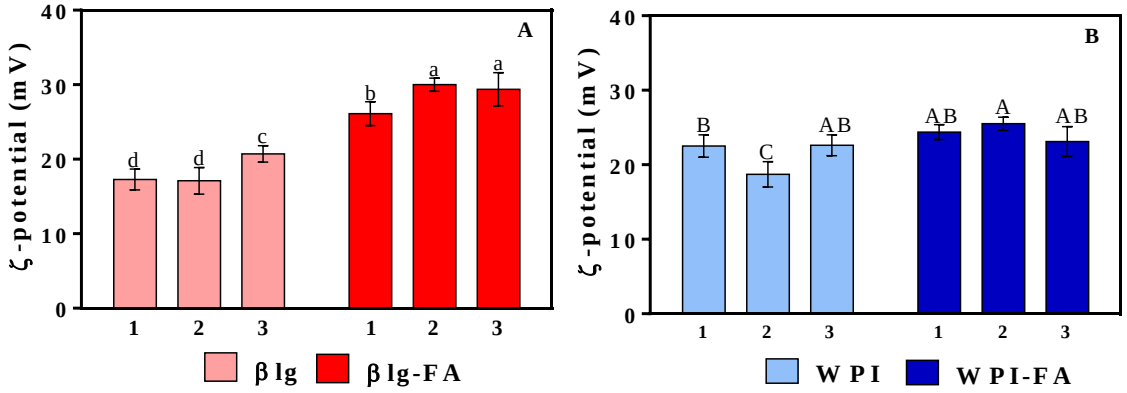

Figure 1: ζ potential of protein components in comparison with protein-FA mixed systems in three concentrations (1: 0.00625%; 2: 0.0125%; 3: 0.01825%), and pH 3.0. A) βlg and βlg-FA; B) WPI and WPI-FA. Different letters indicate significant differences p≤ 0.05. Lowercase letters correspond to the βlg system and uppercase letters to the WPI system.

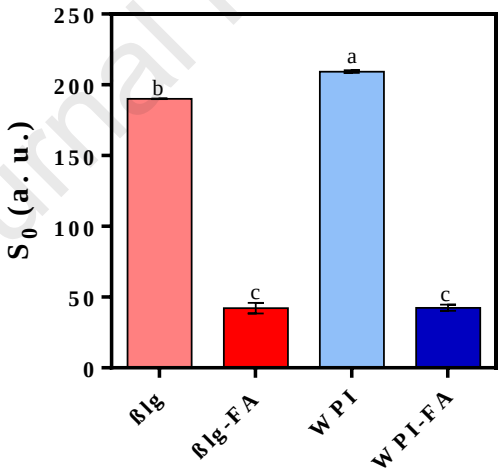

Figure 2. Surface hydrophobicity (S_0) for βlg and WPI in comparison with S_0 for βlg-FA and WPI-FA mixed systems. Different letters indicate significant differences p≤ 0.05.

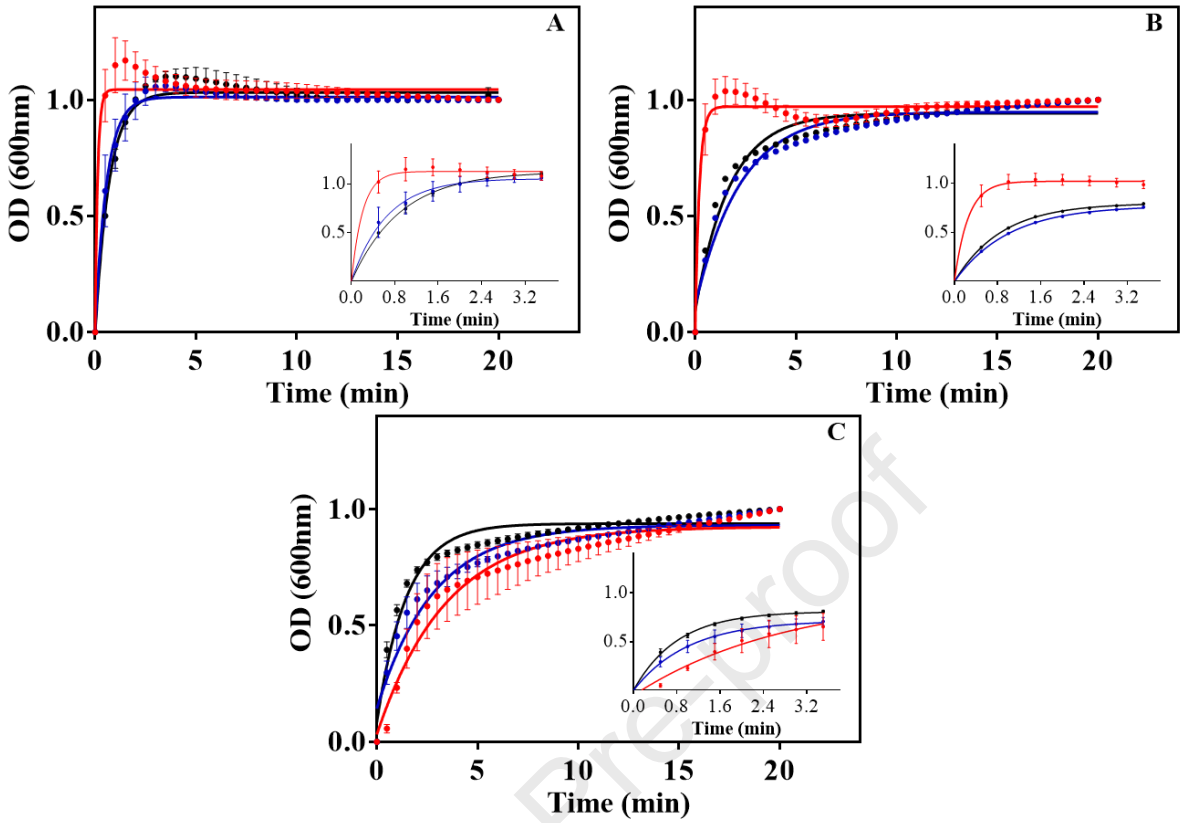

Figure 3. Time dependence of the OD at 600 nm normalized for A) FA; B) βlg-FA and C) WPI-FA, registered in three concentrations (0.00625% (red); 0.0125% (blue); 0.01825% (black)); pH 3.0 and 25°C. The solid lines correspond to the best fit according to **Eq. (1).** The insets show the behavior of OD600 at short time. Error bars are within the symbols.

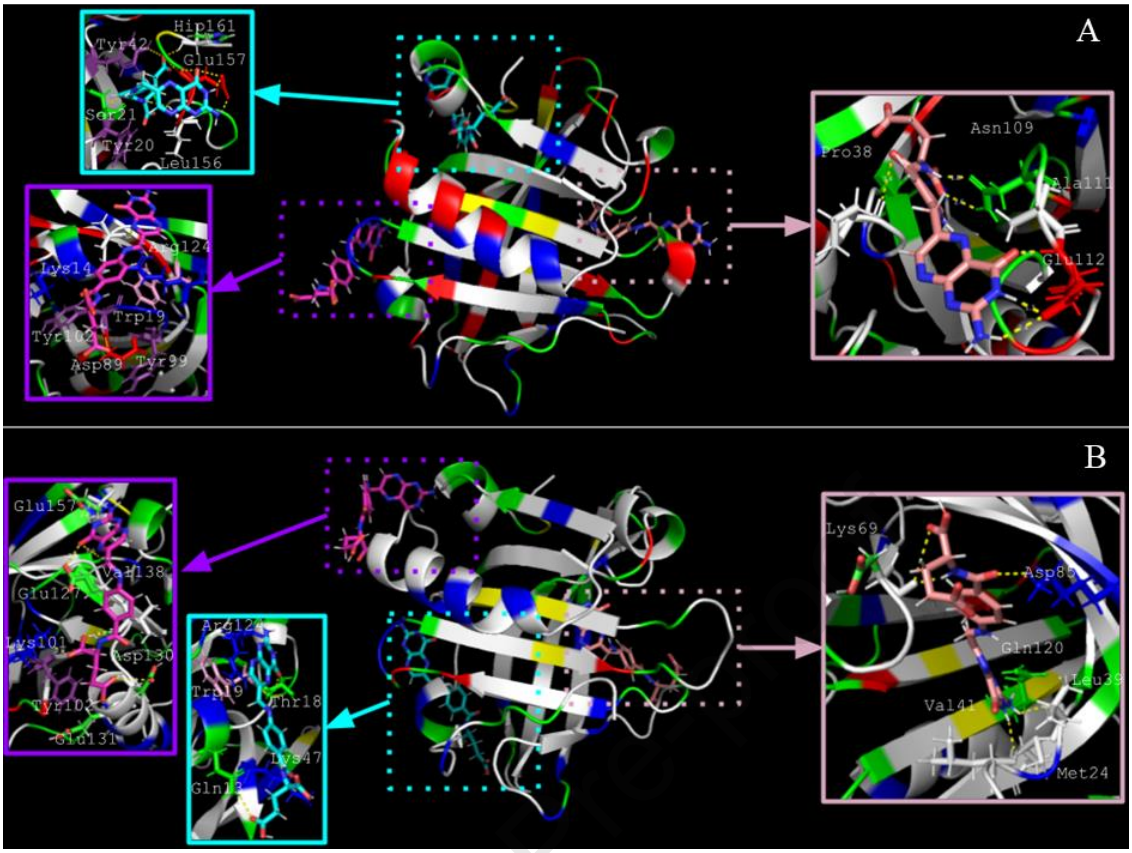

Figure 4: A stereocartoon of the mainchain fold of the most probable protein apo-structure A) at pH 7.0, B) pH 3.0 obtained after docking and MD equilibration. The strands of β-sheet are shown as arrows and the helices as coils. Residues are colored by type: acid (red), basic (marine), polar (green) and apolar (white). The Tyr residues close to the ligand are colored in deep purple, Trp residues in pink. Polar contacts are represented by dotted yellow lines, and residues in contact with ligands are labeled.

ACCEPTED ARTICLE, **FOOHYD 108834**

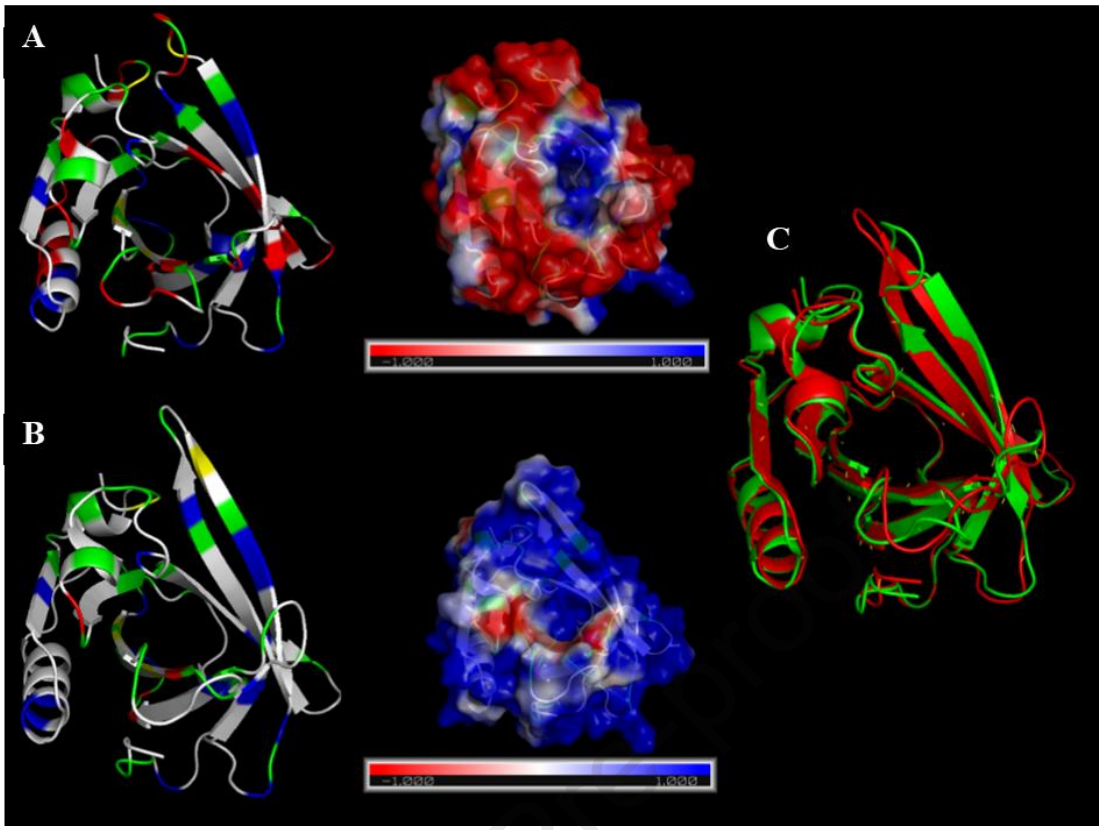

Figure 5: A stereocartoon of the mainchain fold of the most probable protein apo-structure A) at pH 7.0, B) pH 3.0 obtained after docking, MD equilibration. The Adaptive Poisson-Boltzmann Solver (APBS) analysis (Dolinsky et al., 2004) was performed on both structures to obtain a representation of the solvent excluded surface (Connolly surface; min = -1kT/e, max = 1kt/e). The strands of β-sheet are shown as arrows and the helices as coils. Residues are colored by type: acid (red), basic (marine), polar (green) and apolar (white). Figure C) represents an alignment of βlg at pH 7.0 (green) and pH 3.0 (red), showing the rotation of the E-F loop. Yellow dots report unaligned atoms, contributing to a global RMSD of 0.79 A°.

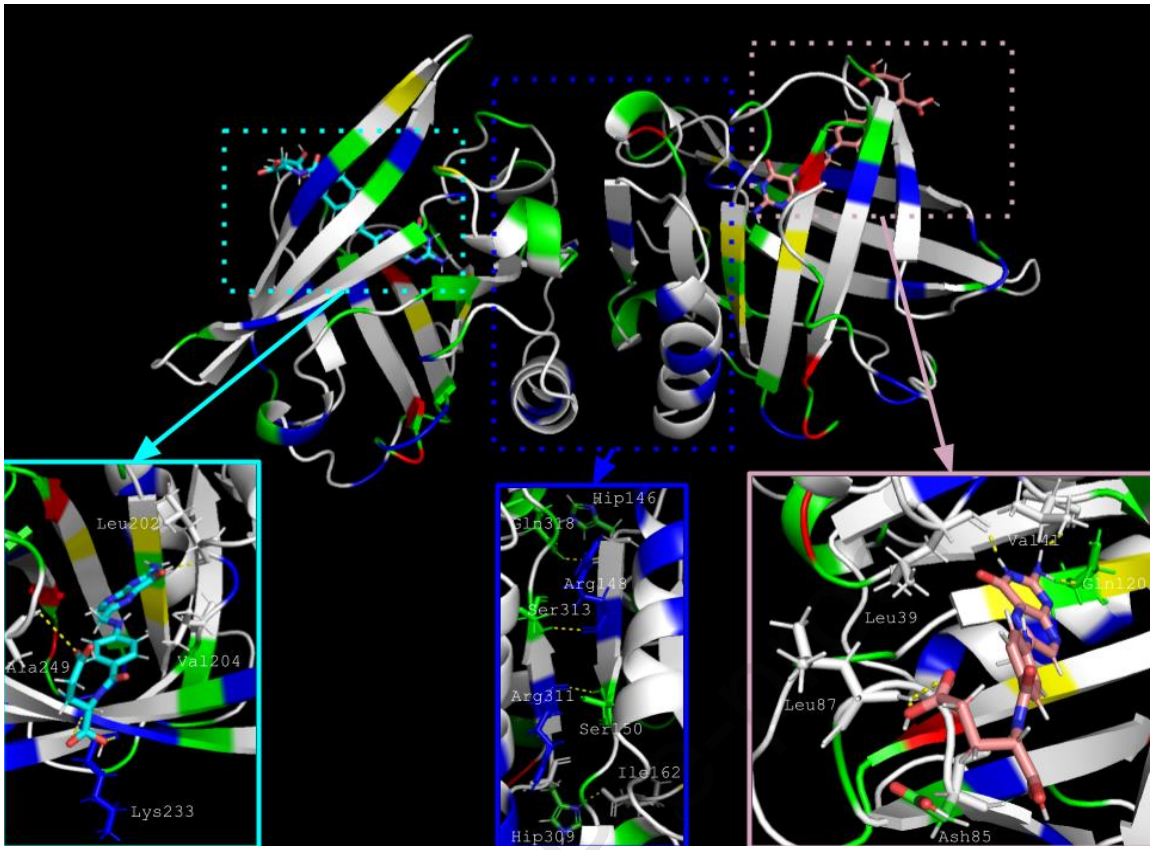

Figure 6: A stereocartoon of the mainchain fold of the most probable protein apo-structure at pH 3.0 obtained after docking and MD equilibration. The strands of β-sheet are shown as arrows and the helices as coils. Residues are colored by type: acid (red), basic (marine), polar (green) and apolar (white). Polar contacts are represented by dotted yellow lines, and residues in contact with ligands are labeled.

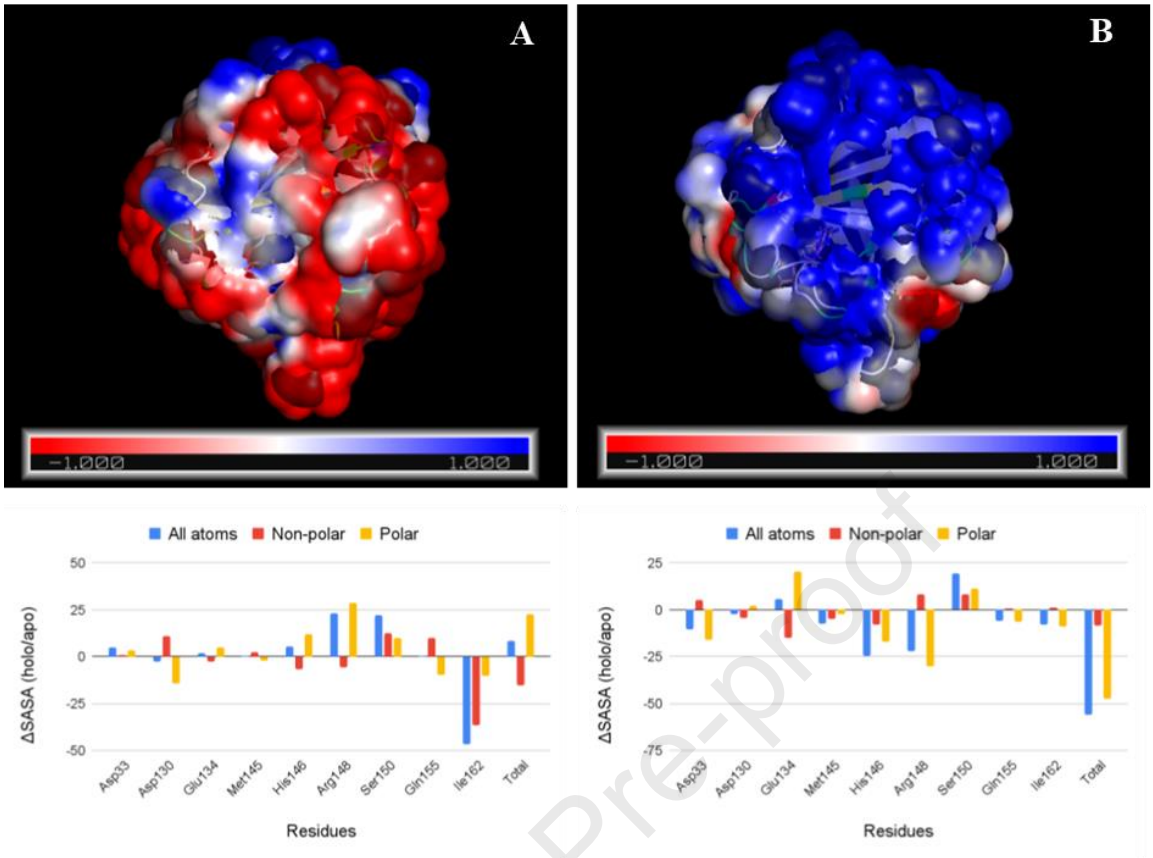

Figure 7: Solvent Accessible Surface Area representation of apo (transparent surface) and holo (solid surface)-monomers (min = -1kT/e, max = 1kt/e) at A) pH 7.0, B) pH 3.0. The ΔSASA (holo-apo) values corresponding to the residues implicated in the dimer interaction are gathered in the graph below each structure.

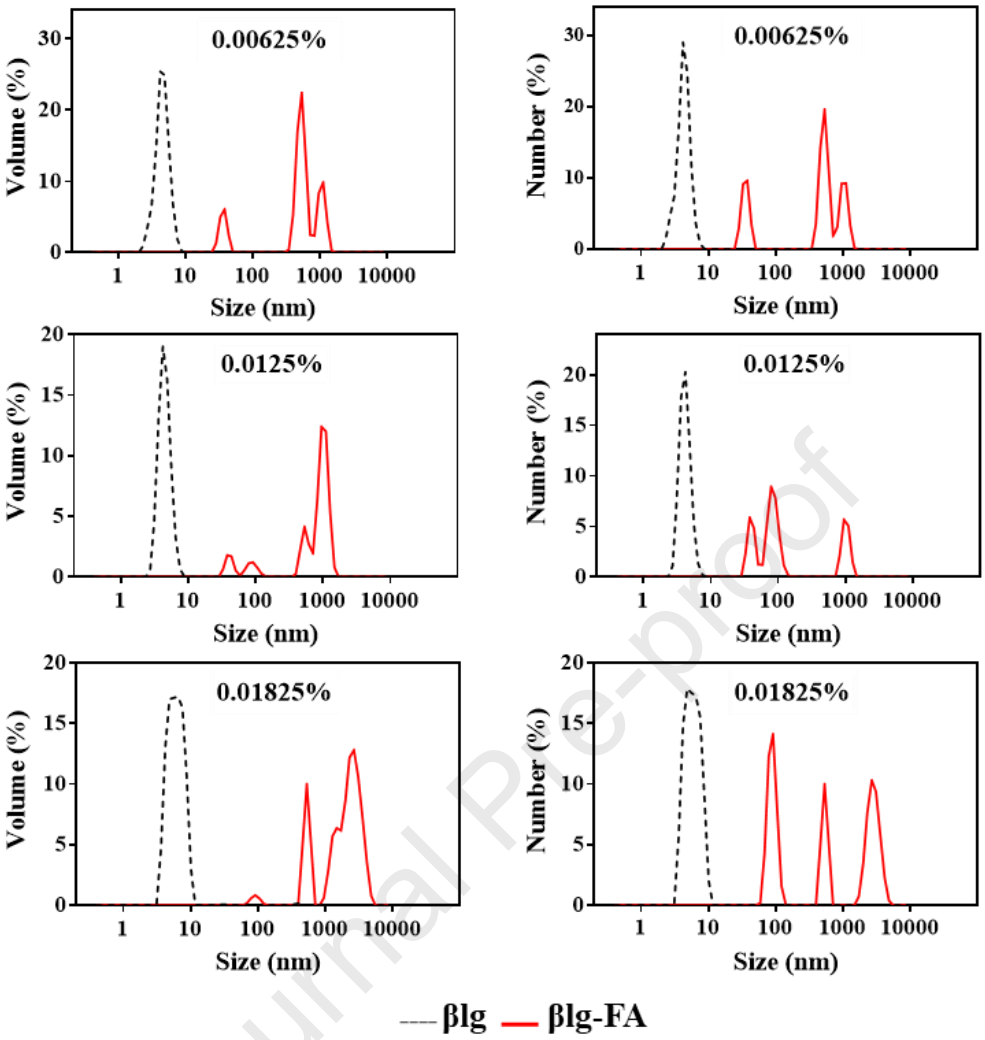

Figure 8: Particle size distribution of βlg protein solutions (dotted lines) and mixed βlg-FA systems (red lines) prepared at pH 3.0 and evaluated at concentrations of 0.00625 g/100g; 0.0125 g/100g and 0.0182 g/100g.

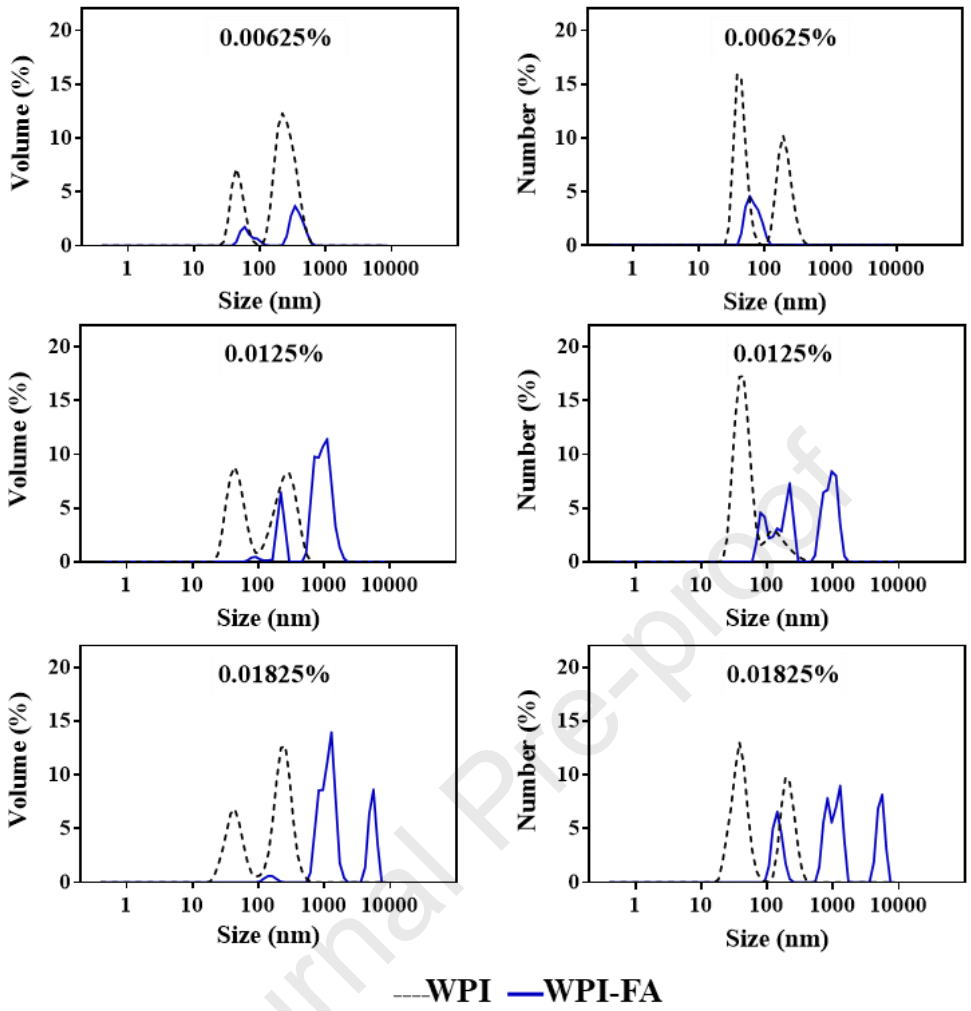

Figure 9: Particle size distribution of WPI protein solutions (dotted lines) and mixed WPI-FA systems (blue lines) prepared at pH 3.0 and evaluated at concentrations of 0.00625 g/100g; 0.0125 g/100g and 0.0182 g/100g.

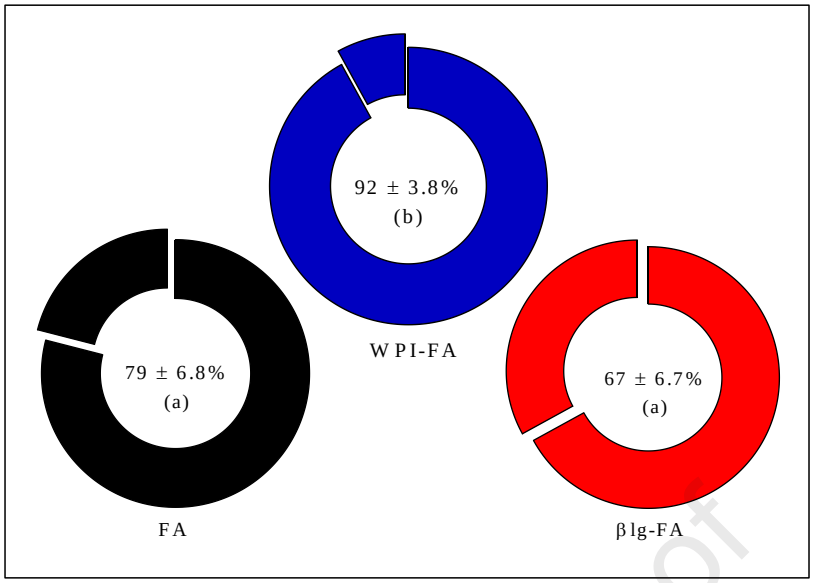

Figure 10: FA bioaccessibility after *in vitro* digestion. The systems concentration was 0.01825% (w/w). Different letters indicate significant differences p≤ 0.05.

HIGHLIGHTS

- ~~WPI and β-lg experimented complexation with folic acid (FA) under acidic conditions.~~
- Complexation process between whey proteins and folic acid were studied at pH 3.0.
- *In silico* and experimental studies suggest hydrophobic interactions were involved.
- βlg dimer structure was stabilized upon binding folic acid at pH 3.0.
- Folic acid induced protein aggregation under these conditions.
- ~~More probable interaction patches of βlg for FA link were determined by bioinformatics tools~~.
- ~~Folic acid resulted bioaccessible as evaluated by *in vitro* digestion.~~
- Folic acid resulted more bioaccessible when carried by the whey protein isolate.

Declarations of interest: The authors have no conflict of interest to declare.